American Mineralogist, Volume 71, pages 277–300, 1986

Phase equilibria and thermodynamic properties of minerals in the BeO-Al_2O_3-SiO_2-H_2O (BASH) system, with petrologic applications

MARK D. BARTON
Department of Earth and Space Sciences, University of California, Los Angeles, Los Angeles, California 90024

ABSTRACT

The phase relations and thermodynamic properties of behoite ($Be(OH)_2$), bertrandite ($Be_4Si_2O_7(OH)_2$), beryl ($Be_3Al_2Si_6O_{18}$), bromellite (BeO), chrysoberyl ($BeAl_2O_4$), euclase ($BeAlSiO_4(OH)$), and phenakite (Be_2SiO_4) have been quantitatively evaluated from a combination of new phase-equilibrium, solubility, calorimetric, and volumetric measurements and with data from the literature. The resulting thermodynamic model is consistent with natural low-variance assemblages and can be used to interpret many beryllium-mineral occurrences.

Reversed high-pressure solid-media experiments located the positions of four reactions:

$$Be_3Al_2Si_6O_{18} = BeAl_2O_4 + Be_2SiO_4 + 5SiO_2 \text{ (dry)}$$
$$20BeAlSiO_4(OH) = 3Be_3Al_2Si_6O_{18} + 7BeAl_2O_4 + 2Be_2SiO_4 + 10H_2O$$
$$4BeAlSiO_4(OH) + 2SiO_2 = Be_3Al_2Si_6O_{18} + BeAl_2O_4 + 2H_2O$$
$$Be_3Al_2Si_6O_{18} + 2Al_2SiO_5 = 3BeAl_2O_4 + 8SiO_2 \text{ (water saturated)}.$$

Aqueous silica concentrations were determined by reversed experiments at 1 kbar for the following seven reactions:

$$2BeO + H_4SiO_4 = Be_2SiO_4 + 2H_2O$$
$$4BeO + 2H_4SiO_4 = Be_4Si_2O_7(OH)_2 + 3H_2O$$
$$BeAl_2O_4 + Be_2SiO_4 + 5H_4SiO_4 = Be_3Al_2Si_6O_{18} + 10H_2O$$
$$3BeAl_2O_4 + 8H_4SiO_4 = Be_3Al_2Si_6O_{18} + 2Al_2SiO_5 + 16H_2O$$
$$3Be_2SiO_4 + 2Al_2SiO_5 + 7H_4SiO_4 = 2Be_3Al_2Si_6O_{18} + 14H_2O$$
$$4BeAlSiO_4(OH) + Be_2SiO_4 + 7H_4SiO_4 = 2Be_3Al_2Si_6O_{18} + 14H_2O$$
$$2BeAl_2O_4 + Be_2SiO_4 + 3H_4SiO_4 = 4BeAlSiO_4(OH) + 4H_2O.$$

The results of these experiments were combined with the heat capacities and entropies determined in a companion study and with data from the literature to estimate the thermodynamic and thermophysical properties of the beryllium minerals. Eighty-six data sets containing over 1000 independent observations were evaluated using the program PHASE20. The values of $G^\circ_{298,1}$ (kJ/mol) and $S^\circ_{298,1}$ (J/(K·mol)) with their uncertainties (2σ) are behoite −827.3(6.7), 45.57(0.18); bertrandite −4300.6(1.6), 172.11(0.77); anhydrous beryl −8500.4(3.8), 346.7(4.7); chrysoberyl −2176.2(1.5), 66.25(0.30); euclase −2370.2(1.1), 89.11(0.40); and phenakite −2028.4(0.9), 63.43(0.27).

The effect of water on the stability of beryl is treated as a purely volumetric interaction

$$G_{P,T,\text{hydrous beryl}} = G_{P,T,\text{anhydrous beryl}} - P_{\text{fluid}} V_{\text{cav}},$$

where V_{cav} is an effective volume for the fluid occluded by the beryl structure (14.1 cm³/mol). Not only does this simple "bottle model" work as well for beryl as alternative, more sophisticated models, in part owing to the lack of hydration data, it also appears to work reasonably well for cordierite.

Beryl has a wide stability range consistent with its relative natural abundance. The stability field of beryl is greatly increased by high fluid pressures and by alkali-containing solid solutions. The assemblage chrysoberyl + quartz is stable only at relatively high temperatures (>600°C) or with $P_{\text{fluid}} < P_{\text{total}}$. At moderate pressures with decreasing temperature, euclase becomes stable around 400°C. Euclase replaces beryl in aluminum silicate–bearing assemblages in the 300°C range. In the 200°C range, phenakite and bromellite hydrate to bertrandite and behoite, respectively, and pure beryl reacts to euclase + quartz + bertrandite or phenakite. The predicted phase relations are in good qualitative agreement

0003–004X/86/0304–0277$02.00

with natural associations. Consideration of the effect of solid solution in beryl improves the agreement.

In most geologic environments, externally imposed chemical potentials govern the stability of beryllium minerals. As a result, minerals in this system are perhaps most useful as indicators of metasomatic variables. Euclase, for example, has a broad P-T stability range, but is stable only in environments with unusually high alumina activities, thus accounting for its relative rarity.

Introduction

Beryllium, one of the geochemically less abundant elements, occurs as an essential component in more than 50 minerals (Fleischer, 1980). Although rarely composing more than a small portion of any rock, beryllium minerals are fairly common, especially in differentiated felsic igneous and related metasomatic rocks. The variety of beryllium minerals and their widespread occurrence mean that they can be useful petrologic indicators.

Of the beryllium minerals, the most common and hence the most petrologically and economically important belong to the system BeO-Al_2O_3-SiO_2-H_2O (BASH). Over twenty phases occur in this system, and those of geologic interest are listed in Table 1. The Al_2O_3-SiO_2-H_2O system has been intensively studied, and its phase relations are well understood (see recent data and reviews by Hemley et al., 1980; Perkins et al., 1979; thermodynamic compilation by Robinson et al., 1982). These studies propose similar phase diagrams for the ASH system and thus provide a reasonable basis for addition of the component BeO.

Relatively few thermochemical data are available for beryllium-bearing phases. In this study, phase equilibrium and solubility experiments were performed to provide the information needed along with data from the literature to derive an internally consistent thermodynamic model for phases in the system. This model, in turn, is used to calculate a petrogenetic grid for the BASH system and reactions in more complex systems. From these calculations, deductions can be made about the petrogenesis of rocks containing minerals in this system.

Figure 1 shows the phases considered in this study projected from water. Of these phases, only beryl has a widely variable composition. The aluminum silicates can accept small amounts of transition metals, and kaolinite, pyrophyllite, and diaspore may contain small amounts of halogens substituting for hydroxyl, but their compositional variations are small. Chrysoberyl can contain substantial iron, chromium, and manganese substituting for aluminum, but in most cases this substitution is small (Vlasov, 1967, Vol. III). Euclase and phenakite are uniformly close to their ideal compositions. Ganguli and Saha (1967) reported that synthetic bertrandite can contain $Be(OH)_2$ considerably in excess of the ideal formula, but analyses of natural bertrandites show no evidence of nonstoichiometry.

Beryl, in contrast to the other phases, exhibits a wide range of compositional variation, as a consequence of two kinds of substitutions: species occupying channel sites and species substituting for the tetrahedral or octahedral cations. The alkalies occur in beryl in amounts up to several weight percent, occupying channel sites with charge balance being accomplished by substitution of other cations in the framework sites and accompanied by adjoining water molecules in the channels (Hawthorne and Černý, 1977). Lithium, in coupled substitution with the channel alkalies, replaced beryllium (Hawthorne and Černý, 1977). Water, in addition to accompanying the alkalies, also occupies the channel cavities in a manner similar to that in cordierite (Schreyer and Yoder, 1964; Aines and Rossman, 1984). Both of these substitutions have a profound effect on the stability of beryl. In addition to the alkalies and water, up to several weight percent of magnesium, manganese, iron, and chromium are found in some beryls. The iron occupies both channel positions and substitutes for aluminum in the octahedral sites, whereas chromium, magnesium, and manganese substitute for the aluminum (Goldman et al., 1978; Nassau and Wood, 1968; Wood and Nassau, 1968; Gibbs et al., 1968). Helium, carbon dioxide, and argon have also been found in beryl (Beus, 1966).

Spectroscopic data on beryl and cordierite suggest that water occupies two distinct positions at low temperatures, one with the H-H vector normal to **c** and "sitting" in the rings between the large cavities (Type II), the other with the H-H vector parallel to **c** and located in the large cavities (Type I, Wood and Nassau, 1968). The abundance of Type II water correlates well with the alkali content; this correlation leads to the suggestion that there is bonding between them (Goldman et al., 1978; Hawthorne and Černý, 1977; Wood and Nassau, 1968). Aines and Rossman (1984) have shown that with increasing temperature these two types of water decrease in quantity with equilibrium partitioning favoring a third state that has the spectroscopic characteristics of a gas (not bonded or oriented on an IR time scale).

Many crystallographic structure refinements have been done on phases in this system (Ross, 1964; R. M. Hazen et al., unpub.). None suggests that there is any disorder among the tetrahedral species. The mineralogic properties of the beryllium minerals were recently reviewed by Burt (1982).

Thermodynamic data have been measured for some of the beryllium phases in this system. Low-temperature heat-capacity measurements have been performed on phenakite by Kelley (1939) and on chrysoberyl by Furukawa

Table 1. Names, abbreviations, and formulas of some phases of geologic interest in the BeO-Al_2O_3-SiO_2-H_2O system

Name	Abbr.	Formula	Name	Abbr.	Formula
Aluminum silicate	Als	Al_2SiO_5	Diaspore	Di	$AlO(OH)$
Andalusite	And	Al_2SiO_5	Euclase	Eu	$BeAlSiO_4(OH)$
Behoite	Bh	$Be(OH)_2$	Gibbsite	Gb	$Al(OH)_3$
Bertrandite	Bt	$Be_4Si_2O_7(OH)_2$	Kaolinite	Ka	$Al_2Si_2O_5(OH)_4$
Beryl	Be	$Be_3Al_2Si_6O_{18}\cdot nH_2O$	Kyanite	Kya	Al_2SiO_5
Beryllite	Bl	$Be_3SiO_4(OH)_2\cdot H_2O$	Phenakite	Ph	Be_2SiO_4
Bromellite	Br	BeO	Pyrophyllite	Py	$Al_2Si_4O_{10}(OH)_2$
Chrysoberyl	Ch	$BeAl_2O_4$	Quartz	Qz	SiO_2
Corundum	Co	Al_2O_3	Sillimanite	Sil	Al_2SiO_5

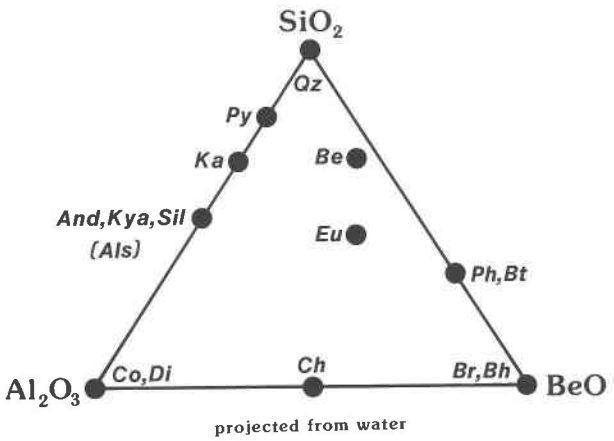

Fig. 1. Minerals in the BeO-Al_2O_3-SiO_2-H_2O system projected from H_2O. Abbreviations from Table 1.

and Saba (1966). Hemingway et al. (1986), in a companion study, measured the low- and high-temperature heat capacities of bertrandite, beryl, chrysoberyl, euclase, and phenakite. Ditmars and Douglas (1967) measured the heat content of chrysoberyl from 298 to 1173 K. Enthalpies of formation of chrysoberyl are available from Robie et al. (1978) and from Holm and Kleppa (1966). Holm and Kleppa (1966), Bamberger and Baes (1972), and Schuiling et al. (1976) gave values for the reaction $2BeO + SiO_2 = Be_2SiO_4$ obtained from oxide-melt calorimetry and phase equilibria. Thermodynamic data for BeO are tabulated in Robie et al. (1978). Kiseleva et al. (1984) reported heats of formation of bertrandite, beryl, chrysoberyl, euclase, and phenakite based on heat-of-solution experiments.

Although there are many studies concerned with synthesis of phases in this system, especially beryl, few have dealt with elucidating the phase relations. In the system BeO-SiO_2-H_2O, Bukin (1967) synthesized bertrandite up to temperatures of 500°C and phenakite at similar and higher temperatures. Ganguli and Saha (1967) performed a number of synthesis experiments in the quaternary system. Beus and Dikov (1967) and Syromatnikov et al. (1971) studied the stability of beryl and other beryllium phases in the presence of alkalies and fluorine-bearing species, but none of their experiments were reversed.

The high-temperature stability of beryl and its melting relations have been investigated by Franz and Morteani (1984), Ganguli (1972), Ganguli and Saha (1967), Miller and Mercer (1965), Van Valkenberg and Weir (1957), and Munson (1967). Unfortunately, these and other studies on beryl and related phases have been synthesis studies and are therefore of limited value in the derivation of thermodynamic properties.

Franz and Morteani (1981), Hsu (1983), and Seck and Okrusch (1972) studied several reactions by reversal experiments. Their data, although limited to only a few reactions, place limits on the upper thermal stabilities of beryl, euclase, and bertrandite. Franz and Morteani (1981) reported a new phase in the quaternary system that is more aluminous than chrysoberyl plus quartz and more silicious than beryl plus andalusite. This phase was not observed in this study and has not been reported by any other investigators, although Miller and Mercer (1965) did synthesize what they believed to be a beryllian mullite in their experiments at higher temperatures.

In addition to the experimental data, a number of compilations of the observed parageneses of beryllium minerals exist (Beus, 1966; Vlasov, 1967, Vols. II and III; Burt, 1978). Burt (1978) derived a detailed topological model for phase equilibria in the system based on natural associations. Burt (1975a, 1975b, 1976, 1980), Franz and Morteani (1984), and Kupriyanova (1982) discussed the stability of these minerals in more complex systems. Franz and Morteani (1981) also discussed the topology of the reactions in the system in light of their experimental results.

Experimental methods and results

High-pressure, solid-media phase-equilibrium and silica-buffering solubility experiments were done to provide the basis for derivation of a thermodynamic model for the BASH system.

Starting materials

Natural materials were used in all the experiments with the exception of synthetic bromellite (1- to 3-mm crystals grown in lithium molybdate flux, NMNH 115234). Cell parameters for the starting materials are listed in Table 2. A cell refinement was not done for BeO because of its toxicity. Crystallographic data were collected by powder-diffraction methods using Ni-filtered Cu $K\alpha$ radiation and were reduced with the program of Burnham (1962). Quartz and corundum served as internal standards.

Partial chemical analyses were performed on an automated ARL-EMX microprobe at the University of Chicago. Spectrometer analyses were done under operating conditions of 15 kV and 15 μA. Data reduction was accomplished using a ZAF-type correction program written by I. M. Steele of the University of Chicago. Standards used were fluor-topaz (for Al, Si, and F in bertrandite and euclase), hematite (for Fe in all but beryl), albite, microcline, pollucite, and synthetic Rb-feldspar (for Na, K, Cs, and Rb, respectively, in the Minas Gerais beryl). Only the chrysoberyl and beryl contain detectable impurities. The chrysoberyl contains 3.1 wt% Fe_2O_3 corresponding to about 2.5 mol% $BeFe_2O_4$. Analyses of the beryl used are given in Table 3. Water contents of the Brazilian beryl and the bertrandite were deter-

Table 2. Crystallographic data for the BeO-Al_2O_3-SiO_2-H_2O starting materials

Material	Cell Parameters[1] a (Å)	b (Å)	c (Å)	β(Å)	V (Å^3)	Source[2]
Andalusite	7.7928(14)	7.8980(19)	5.5539(19)	-	341.83(12)	Black Hills, South Dakota
Bertrandite	8.7192(16)	15.2722(23)	4.5624(17)	-	607.91(16)	Albany, Maine (F.M.N.H. #6969)
Beryl	9.2104(14)	-	9.1903(13)	-	675.18(22)	Robertson Township, Quebec (N.M.N.H. #123207)
Beryl	9.2184(09)	-	9.1678(58)	-	674.70(37)	Minas Gerais, Brazil (provided by R. Gaines)
Chrysoberyl	5.4801(03)	9.4119(07)	4.4288(03)	-	228.43(02)	Colatina, Espirito Santo, Brazil (N.M.N.H. #R15231)
Euclase	4.7703(29)	14.3235(54)	4.6317(39)	100.416(62)	311.26(39)	Minas Gerais, Brazil (N.M.N.H. #121350)
Phenakite	12.4722(10)	-	8.2532(19)	-	1111.82(21)	San Miguel di Piracicaba, Brazil (N.M.N.H. #B21152)
Quartz						unknown (University of Chicago #2099)

[1] Errors given in parentheses (1σ)

[2] N.M.N.H. = National Museum of Natural History, F.M.N.H. = Field Museum of Natural History

mined by loss on ignition (average of 5 samples each). The bertrandite results are consistent with normal bertrandite stoichiometry and limit the substitution of $Be(OH)_2$ for SiO_2 (proposed by Ganguli and Saha, 1967) to <3%. The Quebec beryl was used in the silica-buffering experiments and the Brazilian beryl was used in the high-pressure experiments.

The minerals were separated from impurities by coarse crushing and hand-picking. On examination in oils, both beryl samples were found to have moderately abundant (0.01% to 0.1% by volume) fluid inclusions. The other phases have few inclusions with the exception of the chrysoberyl which contains some oxide inclusions (which may contribute to the observed iron content).

High-pressure experiments

Piston-out piston-cylinder reversal experiments were performed to determine the temperatures as a function of pressure for Reactions 1 to 4:

$$Be_3Al_2Si_6O_{18} = BeAl_2O_4 + Be_2SiO_4 + 5SiO_2 \text{ (water free)} \quad (1)$$

$$20BeAlSiO_4(OH) = 3Be_3Al_2Si_6O_{18} + 7BeAl_2O_4 + 2Be_2SiO_4 + 10H_2O \quad (2)$$

$$4BeAlSiO_4(OH) + 2SiO_2 = Be_3Al_2Si_6O_{18} + BeAl_2O_4 + 2H_2O \quad (3)$$

$$Be_3Al_2Si_6O_{18} + 2Al_2SiO_5 = 3BeAl_2O_4 + 8SiO_2 \text{ (water saturated)}. \quad (4)$$

The starting materials (Tables 2 and 3) for each of these reactions were mixed together in stoichiometric proportion with equal masses of reactant and product assemblages. The mixes were ground under acetone to an average particle size of 5 μm (determined by examination in oil). For Reaction 1, the beryl was dehydrated at 1400°C for 1 h. Although this is above the 1-bar stability limit of beryl (Ganguli, 1972), optical and X-ray examination showed no evidence of decomposition. After grinding, the mixtures were loaded into 6-mm-long platinum capsules. Approximately 2 mg of water were added to each of the capsules for the water-containing experiments. The capsules were sealed by arc welding and folded in half to fit into the pressure assembly. Before sealing, the capsules for Reaction 1 were crimped and placed in an oven at 800°C for several hours to drive off any volatiles acquired during the mixing and loading steps. Devolatilization of the mix could not be done at 1400°C because the starting mix reacted rapidly to give beryl (which should be metastable relative to chrysoberyl + cristobalite + phenakite).

Two pressure assemblies were used. An assembly consisting almost entirely of NaCl was used for the water-bearing experiments which were all conducted below 800°C. This salt assembly has been shown by Holland (1980) to be friction-free within experimental uncertainty. Experiments on Reaction 1, which were conducted between 1150 and 1450°C, used an assembly consisting largely of pyrex glass. The pyrex assembly has an appreciable friction requiring pressure calibration. Consequently, reversals were done on the reaction anhydrous cordierite = sapphirine + quartz. This reaction has been reversed at 1250°C between 7000 and 7500 bars in an internally heated gas apparatus by R. C. Newton (pers. comm., 1980). For the calibration reversals, the cordierite and sapphirine + quartz were prepared in the manner of Newton (1972). Care was taken to ensure that the cordierite-sapphirine-quartz mix was completely dry before sealing the capsules. The "true" position of the reaction at other temperatures can be obtained from the 1250°C bracket and the Clausius-Clatpeyron slope (derived from the thermodynamic data presented by Newton et al., 1974). Table 4 gives the results of the calibration experiments. These experiments and others at higher pressures using this same pressure assembly (Perkins and Barton, unpub.) indicated that the pressure correction is approximately −10%. A pressure correction of −10% was applied to all experiments using the pyrex assembly.

Tungsten-rhenium thermocouples were used for the high-temperature experiments. Chromel-alumel thermocouples were used for the lower-temperature experiments. The position of the thermocouple was checked on dissection of the assembly after each run, and any run in which the thermocouple was more than 1 mm from the capsule was rejected. No pressure correction has been applied to the temperature measurements. Uncertainty in the pressure measurements is estimated to be about 200 bars. The salt-assembly experiments maintained constant pressure after an initial period of expansion that accompanied the attainment of a thermal steady state. The pressure for the pyrex-assembly experiments often drifted considerably with time requiring pressure adjustments over long periods. The estimated precision of the temperature measurements is ±5°C.

For all experiments, reaction direction was determined by comparing X-ray scans of the run products with those of the starting

Table 3. Analyses of the beryls used in the experiments

Oxide	Quebec[1] (N.M.N.H. #123207)	Brazil
SiO_2	65.74	64.2
BeO	14.13	n.d.
Al_2O_3	18.03	17.9
Fe_2O_3	0.44	determined as FeO
FeO	0.25	0.75
Li_2O	0.01	n.d.
Na_2O	0.10	0.92
K_2O		0.21
Rb_2O	0.04	<0.05
Cs_2O	0.16	0.17
H_2O	1.01	1.52[2]
	99.91	

[1] Analysis by R.E. Stevens, provided by M. Fleischer (U.S. Geological Survey).

[2] Determined by loss on ignition.

mixes. The anhydrous charges were well sintered, homogeneous pellets that were quite difficult to grind, whereas the hydrous charges were loose powders of rather coarsely recyrstallized phases. A reaction was considered to have taken place if there was more than a 20% change in the relative peak intensities of phases on one side of the reaction versus the other. If any of the peaks indicated an inconsistent direction of reaction, the run was considered to indicate no reaction. The relative intensities of the peaks for Reaction 4 were sensitive to the degree of grinding. It was possible to change the apparent direction of the reaction from beryl + kyanite to chrysoberyl + quartz with moderate grinding for experiments near equilibrium. As a result, only those experiments for which extent of reaction was strong (peak ratios changed by more than a factor of two) to very strong (peaks of the reactant assemblage nearly gone) were used (determined by XRD after slight grinding). For some runs, grain mounts were made and optically examined, but they were used to determine only the presence or absence of phases and not the direction of reaction. For the water-bearing experiments, only those runs in which water was unambiguously present on opening of the capsule were used.

Table 4 gives the results for Reaction 1 and for the cordierite calibration reactions. The critical experiments for Reaction 1 are plotted in Figure 2 along with the position of the equilibrium calculated from the thermodynamic model presented later. Several experiments conducted on Reaction 1 (Table 4) in the presence of excess water gave complete reaction to beryl in less than 1 d at 700 and 800°C at pressures up to 20 kbar. The uncertainty associated with the impurities in the beryl could have been avoided by using synthetic beryl; however, the ease with which complete yields of medium-grained beryl can be obtained by this method was not discovered until too late in the study.

Results for Reactions 2–4 are given in Table 5 and are plotted in Figures 3–5. These results agree reasonably well with those of Hsu (1983) and Franz and Morteani (1981). The slightly higher temperatures found in this study may be due to the alkali content of the beryl used in these experiments. Franz and Morteani and Hsu used synthetic beryl that presumably was alkali free. As discussed in the Thermodynamics section, the alkali content of beryl should have a significant effect on its stability. The effect of alkalies has been taken into account in the calculated curves for Figures 2–5.

Table 4. Results for beryl breakdown and pyrex-assembly calibration

Run No.	Time (h)	Temp. (°C)	Pressure (kbar) nominal	corrected	Results
$Be_3Al_2Si_6O_{18}$ = $BeAl_2O_4$ + Be_2SiO_4 + $5SiO_2$ dry, pyrex assembly					
Be-159	13.0	1285	5.8-6.2	5.40	weak be
Be-164	17.0	1285	6.5-7.2	6.20	strong ch+ph+qz
Be-165	6.0	1350	5.8-6.2	5.40	moderate be
Be-166	5.5	1350	6.8-7.2	6.30	strong ch+ph+qz
Be-167	20.0	1225	7.3-7.7	6.75	moderate ch+ph+qz
Be-172	4.0	1410	6.8-7.2	5.40	no reaction
Be-175	18.0	1200	6.8-7.2	6.30	weak be
Be-198	4.5	1410	6.4-6.8	5.95	very strong ch+ph+qz
Be-201	4.5	1410	5.6-5.9	5.15	weak be
Be-202	16.0	1250	6.2-6.6	5.75	weak be
Be-204	18.0	1250	6.9-7.2	6.30	no reaction
Be-205	8.0	1450	5.6-5.8	5.15	strong ch+ph+qz
Be-208	18.0	1150	7.0-7.4	6.50	weak be
Be-234	48.0	1150	7.7-8.0	7.05	strong ch+ph+qz
Be-235	3.0	1450	5.5-5.7	5.05	strong be
$Be_3Al_2Si_6O_{18}$ = $BeAl_2O_4$ + Be_2SiO_4 + $5SiO_2$ water-saturated, salt assembly					
Be-137	24.0	825	10.0-10.9	-	complete be
Be-138	20.0	825	15	-	complete be
Be-139	24.0	825	20	-	complete be
Be-140	45.0	725	19.5-20.5	-	very strong be
Cordierite = Sapphirine + Quartz dry, pyrex assembly					
Be-215	10.0	1250	7.9-8.1		no reaction
Be-217	10.0	1250	8.1-8.3		weak cd
Be-218	10.5	1250	7.7-7.9		weak sp+qz
Be-221	4.0	1380	7.8-8.0		very strong cd
Be-227	4.0	1380	8.1-8.3		strong sp+qz

Another possible source of error is that the water content of beryl may not have reached equilibrium values during the experiments. Jochum et al. (1983) found that hydration and dehydration in cordierite proceeds rapidly at temperatures above 400°C and pressures above 1 kbar (times on the order of a few hours or less). It therefore seems likely that beryl achieved an equilibrium water content during the experiments. Alkalies in beryl, however, inhibit dehydration (Ginzburg, 1955) and thus possibly slowed hydration in these experiments.

Silica-buffering experiments

An extensive series of aqueous silica–buffering experiments were performed at 1 kbar on various assemblages from the BeO-

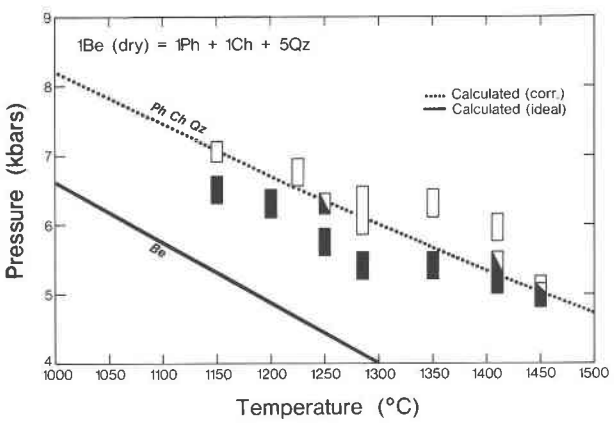

Fig. 2. The dry breakdown of beryl at high temperature. The open rectangles indicate reaction to chrysoberyl + phenakite + quartz, the filled rectangles indicate reaction to beryl, and the half-filled symbols indicate no reaction. The ideal line is calculated for pure beryl; the corrected line takes into account the impurities in the experimental beryl. See the text for details. Abbreviations from Table 1.

Table 5. Results for high-pressure, water-saturated reactions

Run No.	Time (h)	Temp. (°C)	Pressure (bars)	Results
$4BeAlSiO_4(OH) + 2SiO_2 = Be_3Al_2Si_6O_{18} + BeAl_2O_4 + 2H_2O$				
Be-153	96	500	8000	moderate eu + qz
Be-188	48	520	8000	very strong be + ch
Be-191	36	555	10000	moderate be + ch
Be-193	24	590	12000	very strong be + ch
Be-195	24	580	12000	weak eu + qz
Be-199	48	545	10000	moderate eu + qz
Be-200	24	585	12000	no reaction
Be-211	72	480	6000	weak eu + qz
Be-213	96	510	8000	no reaction
Be-216	72	490	6000	weak be + ch
Be-224	21	640	15000	moderate eu + qz
Be-228	20	650	15000	very strong be + ch
$20BeAlSiO_4(OH) = 3Be_3Al_2Si_6O_{18} + 7BeAl_2O_4 + 2Be_2SiO_4 + 2H_2O$				
Be-179	60	580	10000	strong eu
Be-183	36	590	10000	strong be + ch + ph
Be-185	48	550	8000	moderate be + ch + ph
Be-186	24	610	12000	strong eu
Be-192	12	625	12000	moderate be + ch + ph
Be-196	48	540	8000	no reaction
Be-210	48	535	8000	weak eu
Be-214	48	545	8000	no reaction
Be-223	20	665	15000	weak eu
Be-225	20	680	15000	weak be + ch + ph
Be-230	72	500	6000	weak eu
Be-231	72	515	6000	weak be + ch + ph
$Be_3Al_2Si_6O_{18} + 2Al_2SiO_5(Kya) = 3BeAl_2O_4 + 8SiO_2$ (with excess water)				
Be-262	24	775	15000	moderate be + kya
Be-265	120	800	15000	strong ch + qz
Be-269	20	850	16500	strong be + kya
Be-271	20	850	17000	very strong ch + qz

Al_2O_3-SiO_2-H_2O system and from the BeO-SiO_2-H_2O subsystem. In these experiments, the solid-phase assemblage buffers the concentration of aqueous silica in solution. Given a measured silica concentration and the assumption that aqueous silica obeys Henry's law over the concentration range of interest, the equilibrium constant of the reaction (and hence the free energy) can be obtained directly. This method has been used extensively by J. J. Hemley and coworkers in studies of the MgO-SiO_2-H_2O and Al_2O_3-SiO_2-H_2O systems (Reed and Hemley, 1966; Hemley et al., 1977a, 1977b, 1980).

In this study the method has been modified somewhat from that of Hemley et al. (1977a) to permit much smaller samples. Capsules were made from 2-cm lengths of 3-mm-diameter platinum tubing. The tubing was carefully annealed prior to loading

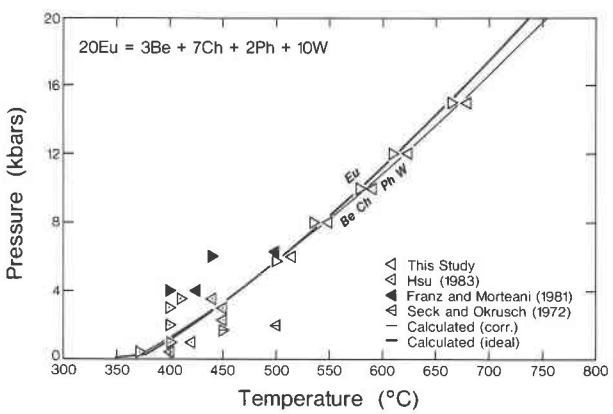

Fig. 3. Experimental results on the breakdown of euclase. The ideal line is calculated for pure beryl; the corrected line takes into account the impurities in the experimental beryl. See the text for details. Abbreviations from Table 1.

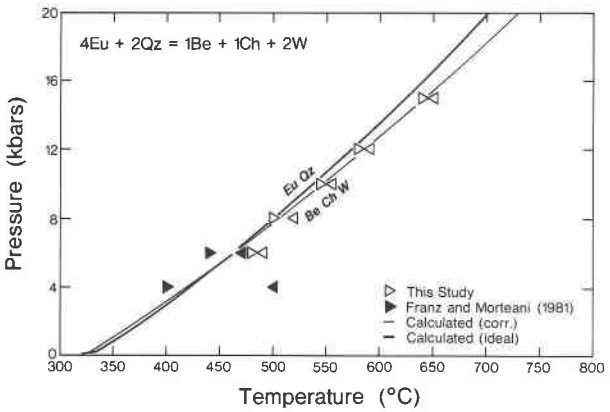

Fig. 4. Experimental results on the breakdown of euclase + quartz. The ideal line is calculated for pure beryl; the corrected line takes into account the impurities in the experimental beryl. See the text for details. Abbreviations from Table 1.

the charge in order to make opening the capsules easier at the end of the experiments. Platinum was used because gold capsules tended to anneal themselves to one another when run together. Charges consisted of 15–35 mg of silica solution or distilled water loaded using a microsyringe and 1–2 mg of the solids that composed the buffering assemblages. After loading, the capsules were crimped shut, the crimped ends clipped straight, and then sealed by arc welding. At each stage the capsules were weighed in order to determine the masses of the reactants and to detect losses. At the end of a run, any capsule that differed by more than 0.15 mg from its prerun weight was rejected. Most capsules varied by less than 0.10 mg.

The powders for the buffering assemblages were prepared by grinding the reagents to coarse powders and then sieving and washing with distilled water to concentrate the 30- to 150-μm size fraction. Bromellite, however, was only coarsely crushed under acetone in a glove bag due to its toxicity. The beryl used in these experiments was not dehydrated.

Distilled water and Ludox (ammonia-stabilized colloidal silica) were used to prepare starting silica solutions of various concentrations. The experiments were "reversed" by starting with silica concentrations on the high and low sides of the equilibrium value. Because aqueous silica is the most abundant—but not the only—species in such solutions, approaching equilibrium from both directions with respect to silica transferred the greatest amount of mass in both directions. In other words, even though analogous buffering reactions involving the solid phases and the aqueous beryllium and aluminum species can be written, the amount of solution and reprecipitation necessary to buffer their concentrations is considerably smaller than that needed to buffer the concentration of silica. Therefore, by forcing the silica values to change substantially from either direction, much more material is dissolved and precipitated than would be necessary to buffer the other species alone. These experiments should then be as close to "true" reversals as many conventional phase-equilibrium experiments in which there are one or more degrees of compositional freedom.

After their preparation the capsules were loaded in groups of four into standard cold-seal bombs. Running four capsules together allowed multiple determinations of the same equilibrium while eliminating the effect of variations in temperature and pressure between runs. Internal chromel-alumel thermocouples were

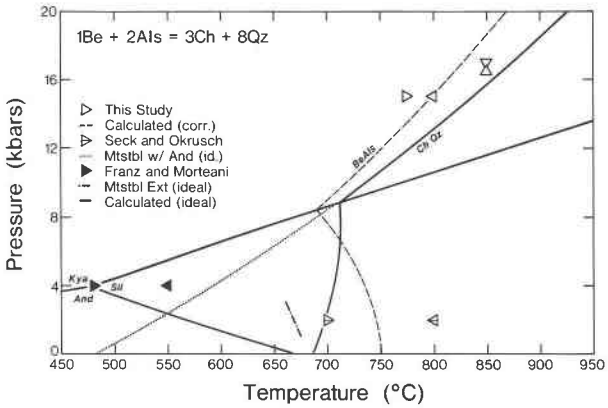

Fig. 5. Experimental results on the water-saturated breakdown of beryl + aluminum silicate. The aluminum silicate phase relations are calculated from the data in Robinson et al. (1982). All the other curves are calculated from the thermodynamic model. The calculated (corrected) curve is for the alkali-containing beryl used in this study. The solid curve that intersects the kyanite-sillimanite reaction is for pure beryl and the stable aluminum silicate polymorph, whereas the dotted and the dot-dash curves are for the metastable reactions with pure beryl appropriate to the experiments Franz and Morteani (1981) and Seck and Okrusch (1972), respectively. Abbreviations from Table 1.

used with the tip of the thermocouple at the midpoint of the capsules. The thermocouples were calibrated against a standard thermocouple which was in turn calibrated against the melting points of NaCl and ice. Temperatures are believed to be accurate to within ±5°. Bourdon tube–type gauges were used to measure the pressures. These gauges were intercalibrated with one another. Calibration was also performed against a new gauge certified by the factory to ±2%. Pressures are believed to be accurate within 4% (40 bars) of the reported values.

Run times varied from a few days at the highest temperatures to over 3 mo at the lowest temperatures. The length of run was determined by experience. In general, the higher the temperature and the smaller the mass of silica that needed to be transferred, the less the time that was required to reach equilibrium.

Quenching was done at constant pressure by cooling the bomb as rapidly as possible with an air blast. A few runs were quenched by immersion of the bomb in water. In all cases the temperature was below 300°C within 30 s of the start of the quench and below 100°C within 2 min. The capsules were then removed from the bomb, weighed, washed, and analyzed.

Analysis consisted of first opening the capsules in distilled water and carefully washing to recover all the charge. The solutions were then diluted to 50 mL with distilled water and analyzed by using the molybdate blue method (Strickland and Parsons, 1972). Although the opening and dilution of the runs was done in glass containers, large variations in silica concentrations between duplicate runs were detected only in a few analyses where NaOH solutions were used in the washing step or where analysis took place more than 1 d after opening. Such runs were rejected. The estimated uncertainty in the molality of aqueous silica is ±0.05 log units. This compares with ±0.02 log units for the experiments of Hemley et al. (1977a, 1977b, 1980) in which the mass of solution was about 50 times larger. Better results could have been obtained using rapid-quench bombs and the microanalytical techniques described by Frantz and Hare (1973).

After many of the runs, grain mounts of the buffer assemblages were examined optically for new phases or for the complete decomposition of the starting phases. The high-temperature limits for experiments on euclase and bertrandite were determined in this manner, although it was usually clear from the silica analyses that something anomalous had happened. No additional phases were observed in any of the experiments. Nothing was detected that might correspond to the "hybrid" phase of Franz and Morteani (1981). None of the assemblages used contained the bulk composition of the "hybrid" phase; even if it is stable it may not have been able to nucleate.

Several of the reactions studied were metastable relative to one or more alternative assemblages; however, careful checking established that in many cases it was possible to maintain the metastable assemblage without nucleation of the stable phase(s) throughout the course of the experiment. Table 6 presents the results for these experiments. The results are plotted in Figures 6–8.

Aqueous silica concentrations measured for two buffers (beryl + chrysoberyl + andalusite, beryl + chrysoberyl + euclase) were consistently below the values predicted using all the other

Table 6. Results for silica-buffering experiments

Run No.	Time (days)	(°C)	log $m_{H_4SiO_4}$ initial	final
$2BeO + H_4SiO_4 = Be_2SiO_4 + 2H_2O$				
Be-38a	14	600	-2.43	-1.86
Be-56a	84	450	-2.30	-2.12
Be-56b	84	450	-1.70	-2.10
Be-60a	14	600	-2.15	-1.83
Be-60a	14	600	-2.15	-1.83
Be-60b	14	600	-1.77	-1.82
Be-67a	29	410	-∞	-2.26
Be-67b	29	410	-1.77	-2.21
Be-70a	6	600	-1.77	-1.79
Be-70b	6	600	-∞	-1.85
Be-76a	61	350	-2.15	-2.43
Be-76b	61	350	-∞	-2.43
Be-88c	28	450	-1.77	-2.09
Be-88d	28	450	-∞	-2.06
Be-130c	15	540	-2.15	-1.93
Be-130d	15	540	-1.77	-1.92
$4BeO + 2H_4SiO_4 = Be_4Si_2O_7(OH_2 + 3H_2O$				
Be-48a	41	350	-2.00	-2.21
Be-48b	41	350	-2.60	-2.30
Be-64a	42	350	-∞	-2.27
Be-64b	42	350	-1.77	-2.14
Be-73a	60	350	-2.15	-2.21
Be-73b	60	350	-∞	-2.22
Be-83a	36	400	-2.15	-1.96
Be-83b	36	400	-2.15	-1.92
Be-83c	36	400	-1.77	-1.98
Be-84d	36	400	-1.77	-1.93
Be-101a	90	310	-2.15	-2.25
Be-101b	90	310	-2.15	-2.30
Be-101c	90	310	-∞	-2.63
Be-101d	90	310	-∞	-2.70
Be-108a	41	450	-1.77	-1.73
Be-108d	41	450	-1.65	-1.73
Be-114a	106	310	-2.45	-2.50
Be-114c	106	310	-2.45	-2.49
Be-114d	106	310	-2.45	-2.54
Be-125a	97	310	-2.45	-2.53
Be-125b	97	310	-2.45	-2.47
$3Be_2SiO_4 + 2Al_2SiO_5 + 7H_4SiO_4 = 2Be_3Al_2Si_6O_{18} + 14H_2O$				
Be-80a	7	600	-1.47	-1.64
Be-80c	7	600	-∞	-1.66
Be-80d	7	600	-∞	-1.64
Be-86a	28	450	-1.77	-1.84
Be-86b	28	450	-1.77	-1.81
Be-86c	28	450	-∞	-1.77
Be-86d	28	450	-∞	-1.77
Be-89a	7	600	-1.47	-1.67
Be-109a	39	450	-1.77	-1.78
Be-109c	39	450	-1.47	-1.78
Be-130a	14	540	-1.77	-1.69
Be-130b	14	540	-1.65	-1.68

Run no.	Time (days)	(°C)	log $m_{H_4SiO_4}$ initial	final
$BeAl_2O_4 + Be_2SiO_4 + 5H_4SiO_4 = Be_3Al_2Si_6O_{18} + 10H_2O$				
Be-55a	83	450	-2.00	-1.72
Be-71a	6	600	-1.47	-1.50
Be-71b	6	600	-∞	-1.49
Be-96b	28	380	-2.15	-1.81
Be-96c	28	380	-1.65	-1.75
Be-96d	28	380	-1.65	-1.76
Be-106a	29	450	-2.15	-1.70
Be-106b	29	450	-2.15	-1.68
Be-106c	29	450	-1.65	-1.72
Be-106d	29	450	-1.65	-1.69
Be-112c	14	600	-1.47	-1.48
Be-112d	14	600	-1.65	-1.47
Be-123a	25	500	-1.47	-1.60
Be-123b	25	500	-1.47	-1.60
Be-124a	25	500	-1.95	-1.59
Be-124b	25	500	-1.95	-1.58
Be-127c	7	600	-1.65	-1.47
Be-127d	7	600	-1.47	-1.48
Be-128c	33	450	-1.65	-1.69
Be-131c	14	540	-1.47	-1.55
Be-131d	14	540	-1.65	-1.54
Be-134c	10	650	-1.65	-1.57
Be-134d	10	650	-1.95	-1.54
Be-134e	10	650	-1.65	-1.48
$3BeAl_2O_4 + 8H_4SiO_4 = Be_3Al_2Si_6O_{18} + 2Al_2SiO_5 + 16H_2O$				
Be-54a	84	450	-2.00	-1.64
Be-69a	30	450	-1.77	-1.58
Be-88a	28	450	-1.77	-1.59
Be-109b	39	450	-1.77	-1.56
Be-109d	39	540	-1.47	-1.55
Be-131a	14	540	-1.35	-1.39
Be-131b	14	540	-1.65	-1.40
$4BeAlSiO_4(OH) + 7H_4SiO_4 + Be_2SiO_4 = 2Be_3Al_2Si_6O_{18} + 16H_2O$				
Be-84a	36	377	-2.15	-1.78
Be-84b	36	377	-1.77	-1.78
Be-85a	36	450	-2.15	-1.75
Be-85b	36	450	-1.77	-1.77
Be-98a	85	385	-2.15	-1.75
Be-98b	85	385	-1.65	-1.76
Be-108a	41	450	-2.15	-1.76
Be-108b	41	450	-1.65	-1.72
$2BeAl_2O_4 + Be_2SiO_4 + Be_2SiO_4 + 3H_4SiO_4 = 4BeAlSiO_4(OH) + 4H_2O$				
Be-94a	86	380	-2.15	-1.86
Be-94b	86	380	-2.15	-1.84
Be-94c	86	380	-1.65	-1.77
Be-94d	86	380	-1.65	-1.75
Be-121d	52	400	-1.65	-1.72
Be-126d	52	400	-1.95	-1.79

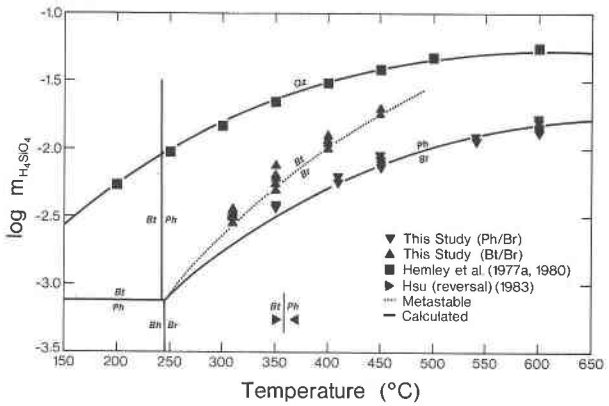

Fig. 6. Silica-buffering results in the BeO-SiO_2-H_2O system at 1-kbar water pressure. The 1-kbar bracket of Hsu (1983) is shown for comparison. Abbreviations from Table 1.

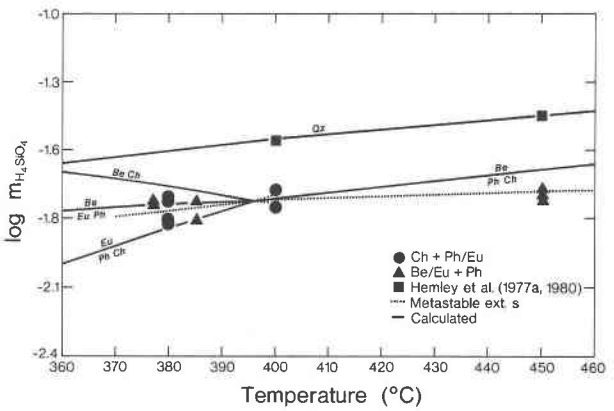

Fig. 7. Silica-buffering results for euclase-bearing assemblages at 1-kbar water pressure. Abbreviations from Table 1.

results (Fig. 6). These two assemblages, which have the highest silica concentrations of those studied, probably precipitated some silica during quench, although no evidence was seen in the grain mounts. Calculations based on the results of Rimstidt and Barnes (1980) support this argument. The 540°C experiments on chrysoberyl + andalusite + beryl were water quenched unlike the others, and perhaps this procedure accounted for their closer approach to the calculated equilibrium. Air-quenched experiments at 600°C scattered widely below the calculated equilibrium value. The results for these two reactions were not used in deriving the thermodynamic properties.

There is a large discrepancy in the position of the reaction bertrandite = phenakite + water between the reversed results of this study using silica buffering techniques and the results of Hsu (1983) using conventional reversal techniques (Fig. 6). Hsu found that the reaction takes place in the mid-300°C range at pressures from 500 to 3500 bars. In contrast, the results here require the temperature of reaction to be less than 300°C, probably in the mid-200°C range. There is no obvious cause for this difference; other results from the two studies on the euclase breakdown reaction agree well (Figs. 3, 7, 8). Both data sets are compatible with the entropy and heat-capacity data on the phases. Several possibilities exist. First, the results of Hsu may represent metastable recyrstallization of bertrandite from finely ground to coarser material at a rate much faster than the (stable) growth of phenakite. This is consistent with the much better cleavage in bertrandite that would tend to make it grind easier than phenakite, but would require that the precipitation of bertrandite from solution be kinetically favored. Bertrandite spontaneously decomposes between 450 and 500°C; previous attempts to determine the reaction have either yielded bertrandite stability limits in this range from synthesis-type experiments (Bukin, 1967; Ganguli and Saha, 1967) or found the growth of bertrandite very difficult to achieve (this study; P. Renders, personal communication, 1984). Hsu's brackets indicate a higher Clapeyron *P-T* slope than predicted by the entropy and volume data; however, because his brackets are wide, a curve can be constructed that is compatible with the calorimetry and all but one of his experiments. A steeper slope might indicate kinetic control of recrystallization which should be nearly independent of pressure (e.g., Wood and Walther, 1983).

An alternative interpretation is that the silica concentrations for bertrandite are too high. This might result from unusually high surface energies on the bertrandite or from unexpected complexes in solution. Surface energies should not have been a problem because the reactants were quite coarse and the reactions could be tightly reversed at 350°C and above. If the pH in the experiments were strongly basic, then significant concentrations of polymeric silica species could have been present. BeO, however, is amphoteric and thus the solutions should have been near neutral. Furthermore, the same effect should have occurred for the phenakite-bromellite assemblage and should not have changed the intersection of the two reactions. Interference of Be-containing species in the analytical method is another possibility, but should be ruled out for the same reason as pH.

There seems no obvious experimental reason to prefer one set of bertrandite results over the other. Free energies of bertrandite are derived using both sets in the following section, and the implications of each are discussed in the Calculated Mineral Stabilities section.

Thermodynamic model

In order to make maximum use of the experimental data from this study and the experimental and calorimetric data from the literature, and then to extrapolate these results to nature, it is necessary to construct a model of the thermodynamic properties of the phases in the BASH system. The derivation of such a model is discussed in this section, along with a review of how it compares with earlier estimates of the thermodynamic properties of minerals in the BASH system. The model is based on a least-squares fit of published phase-equilibrium and calorimetric data and the data presented here. The method of Haas and Fisher (1976) was used. Because water has a significant effect on the stability of beryl, it is first necessary to discuss ways by which the energetic effect of water can be taken into account.

Hydration of beryl

Natural beryl contains up to several weight percent water occurring in the channels in the structure. Other volatile species as well as cations (principally alkalis and alkaline earths) are found in the channels (Beus, 1966; Černý, 1975; Goldman et al., 1978; Hawthorne and Černý, 1977). Similar channel constituents are common in cordierite (Gold-

man et al., 1977; Cohen et al., 1977), and their presence has a major effect on cordierite stability raising the high-pressure stability by several kilobars (Kurepin, 1979; Newton, 1972; Newton and Wood, 1979). Similar results for beryl were anticipated by Burt (1978) and were, in fact, found in this study. The results of several experiments on the hydrous and anhydrous breakdown of beryl (Table 4) demonstrate that the stability field of beryl is greatly expanded by the addition of water. The volume of reaction apparently changes sign for several important reactions (see below). A number of experimental studies have been made on the substitution of volatiles in cordierite (e.g., Mirwald and Schreyer, 1977; Mirwald et al., 1979; Johannes and Schreyer, 1981), but none have been made on the substitution of volatiles or other species in beryl.

The significant effect of channel water on the stability of beryl requires that hydration be taken into account in deriving a thermodynamic model for the BASH system and in discussing the stability relations of beryl in nature. Three hydration models were considered: (1) ideal solution between end-member anhydrous and hydrous beryls; (2) zeolitic water modeled using adsorption isotherms, and (3) a nonenergetic, volume-only interaction ("bottle model").

Newton and Wood (1979) and Kurepin (1979) modeled water-containing cordierite as a solid solution between anhydrous cordierite and a hydrous cordierite of fixed water content. The mixing properties of this solution were assumed to be ideal with the number of sites available for mixing per mole the same as the number of water molecules per mole of the hydrous cordierite end member. This model was examined for beryl because of the structural similarity between beryl and cordierite. Reaction 5 is an analogous hydration reaction written for beryl,

$$Be_3Al_2Si_6O_{18} + nH_2O = Be_3Al_2Si_6O_{18}\cdot nH_2O, \quad (5)$$

where n is the number of moles of water per mole of hydrous beryl. The equilibrium condition for this reaction is given by Equation 6

$$\Delta H^\circ - T\Delta S^\circ + \int_1^P \Delta V\, dP + nRT \ln \frac{X_{HB}}{X_{AB} f_{H_2O}} = 0, \quad (6)$$

where X_{AB} and X_{HB} are the mole fractions of anhydrous and hydrous beryl and the values of n, ΔH°, ΔS°, and ΔV need to be determined for beryl. For beryl, as for cordierite, the volume of the anhydrous and hydrous phases are the same within uncertainty and thus $\Delta V = 0$. Because no hydration data are available for beryl, the water model is constrained only by the effect that varying its parameters has on the internal agreement of the phase equilibria and solubility data. At an earlier stage of this study (Barton, 1981), an iterative fit of this model with other (then available) thermodynamic data gave $n = 1.2$, $\Delta H = -53\,840$ J/mol, and $\Delta S = -136.6$ J/(K·mol). These values fall within the stated uncertainty of the Newton and Wood values for cordierite. It would be difficult to give an absolute uncertainty in these values, but varying any of the parameters by more than 10% gives a considerably worse fit to the experimental data, given the other assumptions necessary. These values produce reasonable agreement with the cordierite hydration data of Mirwald and Schreyer (1977), although they systematically underestimate the water content at low pressures. Newer data on the water contents of cordierite given by Mirwald et al. (1979) suggest that the variation of water with pressure and temperature may be more complex than that predicted by the Newton-Wood hydration model.

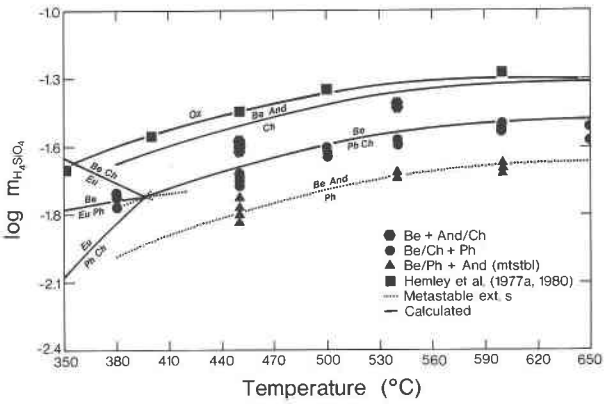

Fig. 8. Silica-buffering results for high-temperature assemblages in the BeO-Al_2O_3-SiO_2-H_2O system at 1-kbar water pressure. See text for discussion. Abbreviations from Table 1.

Martignole and Sisi (1981) evaluated the activity of anhydrous cordierite by Gibbs-Duhem integration of the activity over the pressure ranges of interest. Their technique is similar to those used for evaluating adsorption of water in zeolites. Although their calculations are based on the cordierite hydration data of Schreyer and Yoder (1964), which are probably less accurate than more recent data, the calculations based on the adsorption model are in somewhat better agreement with phase equilibria than are calculations based on the Newton and Wood model. Unfortunately, this technique cannot now be applied to beryl because the required hydration measurements are not available.

An alternative, simple model is to consider the cavities in the beryl (or cordierite) structure as "bottles" that can contain water, but with no energetic effect: the difference in Gibbs free energy between an anhydrous beryl and a beryl saturated with water would be $-V_{cav}(P - 1)$, where V_{cav} is the effective volume of the "bottle." This model predicts that the isohydrons (lines of constant water content) parallel the isochores of water, which is generally consistent with the cordierite experiments. In addition, the simplicity of this model greatly facilitates the application of PHAS20 or similar data-reduction techniques because this model is linearly related to the Gibbs free energy, unlike the first two discussed. One consequence of the bottle model is that the nominally water-free reactions such as Reactions 1 and 7

$$Be_3Al_2Si_6O_{18} + 2Al_2SiO_5 = 3BeAl_2O_4 + 8SiO_2 \quad (7)$$

will be nearly free of curvature because the only change is the addition of a constant volume (although there will be minor curvature resulting from differences in expansivity and compressibility). In contrast, the Newton and Wood (1979) and Martignole and Sisi (1981) models predict substantial curvature at low pressures.

The cordierite hydration data of Mirwald et al. (1979) are somewhat more consistent at low pressures with the ideal-solution model than with the bottle model. A consistency test is not appropriate for the adsorption method because the adsorption isotherms are calculated directly from the hydration data. The bottle model agrees reasonably well with the hydration data of Mirwald et al. (1979) for cordierite at pressures above 1 kbar, excluding their four highest-pressure experiments below 600°C. The calculated V_{cav} for cordierite is 16.2 ± 1.1 cm³ based on 30 measurements (excluding the highest- and lowest-pressure data). The value for all 42 measurements given by Mirwald et al. is 19.2 ± 6.9 cm³. These values compare favorably with 14.1 cm³ estimated here for beryl. The bottle model, therefore, appears to be reasonable for both cordierite and beryl, at least to a first approximation if accurate water contents are not needed at low pressures.

The simplicity of the bottle model is its great advantage; however, there are some observations that are inconsistent with the simplistic interpretation of no energetic interaction. Spectroscopic investigations of water in cordierite and beryl clearly show that there is an energetic interaction between the water and the structure of the mineral (e.g., Aines and Rossman, 1984). Available evidence, however, suggests that the energy of this interaction is low (Langer and Schreyer, 1976; Aines and Rossman, 1984), and thus it should contribute little to the Gibbs free energies of the hydrated phases at moderate to high temperatures and pressures. This contribution could become important at low temperatures and pressures. The somewhat poorer agreement of the calculated phase relations with natural assemblages could be a consequence of this interaction (see following sections) as could the differences between the model and the cordierite hydration data. The molecular sum of alkalis and water commonly exceeds 1.0 per formula unit in alkali-rich natural beryls (e.g., Beus, 1966) further demonstrating that the simplistic volume-for-volume replacement relationship hypothesized here cannot be correct in detail. Lacking experimental constraints on the hydration of pure and alkali-bearing beryl, however, the development of more elaborate hydration models would be purely speculative.

Beryl hydration is accommodated in thermodynamic calculations by adding an additional water volume to the volume of reaction. This formulation should hold for other volatile (noninteracting or weakly interacting) components in the beryl structure. It is clear that for volatile-saturated systems, the whole volume should be added and that for volatile-free systems, no cavity volume should be added. The case of $0 < P_{fluid} < P_{total}$ requires discussion. The effective volume for fluid-undersaturated cases is $V_{cav}P_{fluid}/P_{total}$. This can be seen by imagining a reaction taking place in a system with an osmotic membrane permeable only to the fluid. The *total* volume of reaction will include V_{cav}, but in calculating the Gibbs free energy change from the standard state, the ΔV_{solids} will be integrated from 1 to P_{total}, whereas V_{cav} will only be integrated from 1 to P_{fluid}. Then, to the extent that V_{cav} is independent of pressure, the contribution to ΔG from the fluid will be $V_{cav}P_{fluid}$.

The effect of water on the stability of beryl is considerably more pronounced than the effect of water on the stability of cordierite. This is because in cordierite-breakdown reactions, an increase in aluminum coordination generally leads to a large volume of reaction favoring the stability of the high-pressure phases, whereas, in beryl-breakdown reactions, there is no aluminum-coordination change and consequently a smaller ΔV_{solids}. This is illustrated by two reactions: the breakdown of beryl to chrysoberyl, phenakite, and quartz (Reaction 1, discussed above) and Reaction 7. Figure 9 shows calculated curves for Reaction 7 for $P_{H_2O} = P_{total}$, $0.5P_{total}$, and 0. Decreasing water pressure reduces the stability of beryl + aluminum silicate by several hundred degrees at moderate pressures. This decreased stability results from an approximately 90° change in the Clapeyron slope at any pressure. Differences in the predicted low-pressure phase equilibria might provide a way to test the difference between the alternative hydration models.

Application of PHAS20

The program PHAS20 (Haas and Fisher, 1976) utilizes a weighted least-squares method to enable simultaneous estimation and correlation of the thermodynamic properties of related phases. Data that can be evaluated by the program included heat capacities, heat contents, entropies, volumes, compressibilities, expansivities, heats of reaction, free energies of reaction (e.g., from phase equilibria), and EMF voltages. Other types of data can be incorporated by means of user-written subroutines if they can be related to the underlying functions in a linear way. The BASH system is well suited for application of PHAS20. Eighty-six data sets containing more than 1000 independent observations were used. The data sets include all data types except EMF. The system is greatly overdetermined for the seven species of interest and therefore suitable for a least-squares fitting procedure.

Linear programming methods represent an alternative way to extract thermodynamic properties from a large set of experimental data (e.g., Halbach and Chatterjee, 1984). These methods have the advantage of treating reversal experiments as the inequalities that they are (in ΔG), whereas regression methods are better suited to data that have a regular distribution about the true value (e.g., calorimetric results, solubilities). In this study, only regression techniques were used, although the ideal solution might combine a weighted linear programming method for phase-equilibrium reversal data with a regression technique for other data. Reversal brackets were treated independently with each half-bracket included in the data

set weighted by its P-T estimated accuracy. This results in a relatively even weight being applied throughout the interval between the brackets (Demarest and Haselton, 1981) and thus should help minimize unjustified bias toward the midpoints of the brackets in the final fit.

The data of Robinson et al. (1982) for phases in the ASH system were accepted as fixed values for the evaluation of the thermodynamic properties of the beryllium phases. The data for BeO given in Robie et al. (1978) were also used without modification. Free energies of water at elevated temperatures and pressures were calculated from a program based on Haar et al. (1979, 1981). All other parameters were allowed to vary including the Gibbs free energy of aqueous silica at 1 kbar.

The available heat-capacity, heat-content, and calorimetric-entropy data were fit first without employing any of the other data. The volumetric data also were fit independently. The results for the heat capacities and volumes were then fixed in the preliminary fitting of the phase-equilibrium and heat-of-reaction data. This prevented the program from diverging. Following the preliminary fit, all the regressed terms were allowed to vary to obtain the final fit. A few data were rejected in the process as it became apparent that they were inconsistent with the bulk of the information. It is possible to justify these exclusions in all but one case. The data were all weighted in the regression by the author-reported uncertainties.

Results and discussion

In this section, the derivation of the thermodynamic properties and their agreement with other thermodynamic data are discussed. The thermodynamic model reproduces most of the experimental results within stated uncertainties; calculated phase relations based on the model are in good agreement with observations on natural assemblages. Comparison of the predictions of the model with natural assemblages, however, is deferred to the next section.

The thermodynamic properties from the final PHAS20 fit are summarized in Table 7. The thermophysical properties are summarized in Table 8. RECKON, a Fortran program written by John Haas (U.S. Geological Survey), was used in conjunction with PHAS20 to provide estimates of the errors in the thermodynamic properties. Hemingway et al. (1986) have provided more complete tables for the thermochemical properties of the beryllium minerals.

Volumetric data. Thermal expansivities and compressibilities were incorporated in the model. Data for phases in the ASH system were taken from Robinson et al. (1982). Hazen et al. (1983, personal communication) determined volumes of bertrandite, beryl, bromellite, chrysoberyl, euclase, and phenakite as functions of pressure at room temperature. The compressibility of behoite was estimated from the data for bromellite. Expansivity data for beryl were obtained from Schlenker et al. (1977), for bromellite from Skinner (1966), and for chrysoberyl from Woolfrey (1973) and Cline (1979). Thermal expansivities for behoite, euclase, and phenakite were estimated from the data for bromellite. All the volumetric data were consistent with the final model within 0.2%, nearly all within 0.1%.

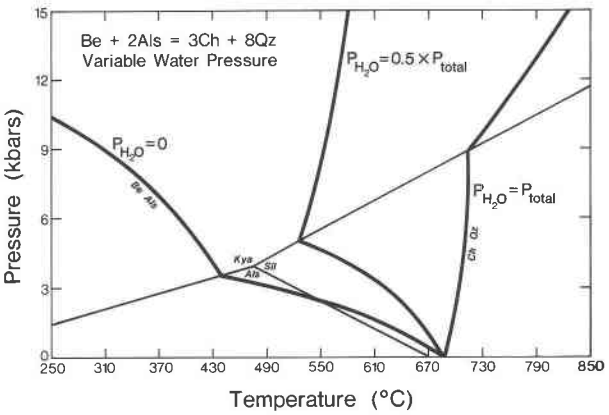

Fig. 9. The low-temperature stability limits of chrysoberyl + quartz at water pressure equal to different fractions of the total pressure. See the text for details. Abbreviations from Table 1.

Heat-capacity and third-law entropy data. Hemingway et al. (1986) determined the heat capacities and third-law entropies of bertrandite, beryl, chrysoberyl (only high-temperature heat capacity), euclase, and phenakite by combined adiabatic and differential scanning calorimetry; they discussed the compositional corrections applied to the data for beryl and chrysoberyl. Furukawa and Saba (1966), Kelley (1939), and Kostryukov et al. (1977) measured the low-temperature heat capacities and calculated the third-law entropies of, respectively, chrysoberyl, phenakite, and behoite. High-temperature heat capacities for behoite were taken from the compilation of Stull and Prophet (1974). Ditmars and Douglas (1967) determined the heat content of chrysoberyl from 273 to 1173 K. Because all the heat-capacity measurements were done at 800 K or less, it proved necessary to estimate values between 800 and 1500 K so that the fitted polynomials varied smoothly in that range. This was done using an extrapolator method developed by G. R. Robinson, Jr. (U.S. Geological Survey), and by oxide sum methods (Helgeson et al., 1978). All the heat-capacity and entropy data fell within two (author-reported) standard deviations of the measurements in the final fit.

Silica-buffering data. For the silica-buffering reactions, standard Gibbs free energies of reaction were calculated from the relation

$$\Delta G^\circ_T = -RT \ln m^n_{H_4SiO_4} f^s_{H_2O} + \int_P^1 (\Delta V_{solids} + bV_{cav})\, dP, \quad (8)$$

where $m_{H_4SiO_4}$ and n are the molality and stoichiometric coefficient of aqueous silica, f_{H_2O} is the fugacity of water at the temperature and pressure of the reaction, s is the stoichiometric coefficient of water, b is the stoichiometric coefficient of beryl, and ΔV_{solids} and V_{cav} are, respectively,

Table 7. Thermochemical properties of some phases in the BeO-Al_2O_3-SiO_2-H_2O system

Phase Name	$G^*_{298K,1bar}$	S_{298K}	Cp** a	b	c	d	e	V_{298}	Source G	S	Cp	V
	J/mol	J/K-mol			J/K-mol			J/bar				
Andalusite	-2444564 (456)	91.49 (0.35)	510.336	-0.19180	1.66755	6.45249	-6117.20	5.156 (0.016)	1	1	1	1
Behoite	-827288 (6734)	45.57 (0.18)	249.017	-0.02676	2.02574	-	-3482.74	2.220 (0.011)	4	4	4	6
Bertrandite	-4300625 -4306375 (1629)	172.11 (0.77)	825.336	-0.09966	3.66217	-	-10570.3	9.150 (0.001)	3 9	7	3	8
Beryl (anhydrous)	-8500360 (3796)	346.73 (4.73)	1625.84	-0.42521	6.82544	0.12032	-20180.9	20.355 (0.004)	3	7	3	8
Bromellite	-580078	13.77	69.936	0.00018	-0.67671	-	-635.740	0.8309	2	2	2	2
Chrysoberyl	-2176161 (1481)	66.25 (0.30)	362.701	-0.08353	-0.06798	2.24819	-403.369	3.444 (0.001)	3	2	3	8
Corundum	-1582326	50.94	238.320	-0.04127	0.04728	0.94196	-2561.61	2.560	1	1	1	1
Diaspore	-921432 (403)	35.34 (0.10)	155.894	-0.00340	0.29021	-	-1812.22	1.776 (0.017)	1	1	1	1
Euclase	-2370166 (1084)	89.11 (0.40)	532.920	-0.15373	2.19760	4.12232	-6720.30	4.702 (0.001)	3	7	3	8
Water (ideal gas)	-228611	188.73	10.4831	0.02596	-1.31077	-4.46885	299.188	2479.0	1	1	1	1
H_4SiO_4 (1 M, 1 Kbar)	-1292370	345.09	4465.24	-2.15187	-	-	-72922.1	-	3	3	3	-
Kaolinite	-3799611 (982)	205.15 (0.47)	749.175	-0.13542	1.49195	-	-8278.64	9.949 (0.034)	5	1	1	1
Kyanite	-2445577 (487)	82.41 (0.30)	634.515	-0.20041	1.91390	6.69583	-6561.91	4.421 (0.023)	1	1	1	1
Phenakite	-2028387	63.43 (0.27)	428.492	-0.09958	2.08263	1.98865	-5670.47	3.717 (0.001)	3	7	3	8
Pyrophyllite	-5268625 (807)	239.33 (1.022)	1094.40	-0.32990	4.01105	11.4631	-13075.0	12.764 (0.015)	1	1	1	1
α Quartz	-856306	41.51	83.2575	0.02196	-	-	-778.110	2.259	1	1	1	1
β Quartz	-855777	37.68	58.9128	0.01039	-	-	-	2.295	1	1	1	3
Sillimanite	-2442060 (500)	95.58 (0.33)	592.346	-0.26236	2.73570	9.43392	-7429.77	5.002 (0.002)	1	1	1	1
Vdummy	-	-	-	-	-	-	-	1.412 (0.243)	-	-	-	3

*Errors given here are 2σ for free energies of reaction from the oxides for all phases except the oxides.

**$Cp = a + bT + c \times 10^6 T^{-2} + d \times 10^{-5} T^2 + eT^{-0.5}$

[1]Robinson et al. (1982) [2]Robie et al. (1978) [3]This study [4]Stull and Prophet (1974) [5]Haas et al. (1980)

[6]Seitz et al. (1950) [7]Hemingway et al. (1986) [8]Hazen et al. (in prep.) [9]This study, based on Hsu (1983).

the volume change of the solids in the reaction and the volume of the cavity. H_4SiO_4 is used as the aqueous silica species because it is the one most commonly accepted (e.g., Hemley et al., 1977a). The actual identity of the species is not needed in the modeling as long as the activity coefficient of aqueous silica is constant over the concentration range of interest. This assumption is reasonable for neutral species in aqueous solutions of low to moderate concentrations. In this study the thermodynamic properties of aqueous silica were constrained by the experimentally determined quartz solubilities of Hemley et al. (1977a, 1980). Their values are quite similar to the statistical fit by Walther and Helgeson (1977) to much of the earlier silica solubility work. Only the data of Hemley and others were used in the least-squares fitting in order to maintain consistency with the data of Robinson et al. (1982) on the ASH system. Aqueous silica can then be eliminated from all the reactions by adding the Gibbs free energy of Reaction 9

$$SiO_2 \text{ (quartz)} + 2H_2O = H_4SiO_4 \qquad (9)$$

thereby converting the free energies of the aqueous silica reactions to Gibbs free energies of quartz-bearing reactions.

A correction for solid solution in the experimental beryl was applied to the free energies of the silica-buffering reactions. This correction has a trivial effect on the fit and the calculated curves. Several sets of silica-buffering results were not used in the final fit. These include the data for the beryl + chrysoberyl + andalusite and beryl + chrysoberyl + euclase experiments discussed under Experiments. Also eliminated were some experiments at 310°C on the bertrandite + bromellite buffer. Only those experiments that started near the final silica value were used. The other experiments, which started much farther away from equilibrium, did not converge sufficiently to provide good estimates of the equilibrium values. The final model agrees well with all the silica-buffering results except for the two silica-rich reactions mentioned above.

Phase-equilibrium data. Free energies of reaction for the high-pressure experiments were extracted using the relation

$$\Delta G^\circ_{T,1} = -RT \ln f^s_{H_2O} + \int_P^1 (\Delta V_{solids} + bV_{cav})\, dP. \qquad (10)$$

The symbols are the same as for Equation 8. The Gibbs free energies for the beryl-bearing reactions done in this study were corrected for slight decreases in the activity of beryl due to solid solution in the starting materials and for the portion of the cavity volume occupied by alkalis and thus unavailable to water. The activity correction amounted to 1.8 J/(K·mol) ($= R \ln a_{beryl}$) for the Brazilian beryl and 0.5 J/(K·mol) for the Quebec beryl. Ideal mixing was assumed in the activity calculations, with the cations (Table 2) mixing on sites consistent with the crystal-structure data (Hawthorne and Černý, 1977). The combination of these two factors accounts for the crossing at about 4 kbar of the calculated "ideal" and "corrected" curves in Figures 3 and 4. This crossing implies that the reversed beryl-bearing reactions determined in this study are slightly metastable relative to the reactions in the pure system. Decreasing the entropies and the volumes of these reactions (i.e., treating the beryl as if it were pure) degrades the fit of the data and predicts unrealistically low values for V_{cav}. It is the prediction of an unrealistically low cavity volume that is the main reason for including the compositional correction. This correction, however, is probably well within the total uncertainties, and thus it is retained even though it leads to what must be an imperfect interpretation of the true phase relations.

The value of V_{cav} was allowed to vary with only loose constraints applied (the value was estimated for the purposes of the refinement as 20 ± 10 cm^3). This value was chosen because it is consistent with the range of water contents observed in natural beryls and cordierites and the amount found to enter cordierite in experiments. The thermal expansion and compressibility of V_{cav} were constrained to equal those of beryl. The final estimate (14.1 cm^3) is consistent with maximum water contents of about one mole water per mole of beryl, somewhat less than that found for cordierite and that predicted for beryl using the Newton and Wood model (Barton, 1981).

The results agree reasonably well with the data of Franz and Morteani (1981) and Hsu (1983) on euclase-bearing reactions that were used in the fit. Because the "hybrid" phase was not observed in this study, direct comment cannot be made on its stability. The phase appears to be metastable for several reasons. The phase has not been reported from nature although appropriate bulk compositions exist. Also, the field of occurrence for the hybrid phase shown by Franz and Morteani cannot be a stable field even considering only their other experimental results.

Franz and Morteani (1981) and Seck and Okrusch (1972) did experiments on Reaction 4. Their results, taken together, indicate that this reaction under water-saturated conditions has a low negative slope (Fig. 3). A negative slope in the kyanite field is incompatible with the results of this study (Fig. 3) and with the calculated ΔV. The accuracy of the other determinations is not clear—Seck and Okrusch may not have reversed their reaction; in this study the direction of reaction was found to be difficult to determine by X-ray diffraction methods—hence, they were not heavily weighted in the refinement. These results and Hsu's (1983) bertrandite experiments were the only data that could not be made consistent with the model or justifiably eliminated from consideration.

Table 8. Thermophysical properties of some phases in the BeO-Al_2O_3-SiO_2-H_2O system

Phase Name	Coefficients for Volume Equation*				
	a	b	c	d	e
Andalusite	50.0729	0.00173719	0.536253	-0.00002170	0.7700380
Behoite	21.8476	0.00073054	0.372510	-0.00000890	-
Bertrandite	90.0311	0.00301037	1.534901	-0.00008510	-
Beryl	202.7476	0.00138606	1.529589	-0.00013287	-0.1797429
Bromellite	8.2167	0.00027296	0.139211	-0.00000421	-0.0541870
Chrysoberyl	33.6087	0.00024292	-0.165870	-	0.8221744
Corundum	25.2017	0.00065552	-	-0.00000603	0.2011490
Diaspore	17.4058	0.00118889	-	-0.00003672	-
Euclase	46.2613	0.00154872	0.795689	-0.00003360	-
Kaolinite	98.4196	0.00356979	-	-0.00040442	-
Kyanite	42.3174	0.00124871	0.229753	-0.00000804	1.4324300
Phenakite	36.6712	0.00122702	0.631233	-0.00002525	-0.0978410
Pyrophyllite	126.8190	0.00173097	0.815952	-0.00000725	-
α Quartz	22.1819	0.00135725	-	-0.00004270	-
β Quartz	23.5794	-	-	-0.00004731	-
Sillimanite	49.1338	0.00093571	0.423863	-0.00002614	0.4486300
Vdummy	14.2420	0.00010422	0.120800	-0.00000936	-0.0138458

*V = a + b x T + c x exp(-T/300) + e x exp(-P/35000) (T in K, V in cm^3)

Several factors probably contribute to discrepancies between the thermodynamic model and the phase-equilibrium data. The most important is almost certainly the inadequacy of the simple beryl hydration model to fully account for the energetic contribution of water and other volatiles. This is illustrated by the relatively poor fit of the model to the reversals for Reaction 4 (Fig. 3). Reaction 4 is nominally independent of water and has only a small ΔV_{solids} and ΔS; therefore the calculated position of the equilibrium is sensitive to V_{cav}. The calculated slope for Reaction 4 could be brought into agreement with the results of this study by changing ΔV by +0.4 J/bar. Errors of this magnitude could result from either uncertainty in V_{cav} or in the volumes of the phases (the total volume for one side of the reaction is about 29 J/bar). An additional energy contribution from the interaction of water with the beryl framework is another possibility, as suggested in cordierite by the higher-than-predicted (bottle model) water contents at low pressures and the ordering found by spectroscopic studies.

The phase-equilibrium experiments of Hsu (1983) on the reaction bertrandite = phenakite + water and the silica-buffering results reported here are inconsistent. Possible reasons for this were discussed under Experiments. The values in Table 7 represent individual fits to two sets of data using the calorimetric entropy and heat capacities. The Gibbs free energy of bertrandite given in Table 7 is 1000 kJ more negative than the least-squares fit. This result is still well within the experimental uncertainty and gives more reasonable breakdown temperatures (about 15°C higher).

On the basis of synthesis experiments, Ganguli (1972)

suggested that at 1 bar, beryl becomes unstable relative to chrysoberyl + phenakite + cristobalite between 1300 and 1400°C. The equilibrium temperature predicted from the data in Table 7 and Robinson et al. (1982) is about 970°C. The large difference may be because Ganguli's synthesis experiments did not approach equilibrium. Ganguli's results were not used in the data reduction.

Heat-of-solution and other data. Free energies of reactions involving phenakite are presented by Schuiling et al. (1976) and by Bamberger and Baes (1972). Schuiling et al. (1976) did a series of half-reversals at 1000 K involving phenakite, bromellite, and several other oxides and orthosilicates. They estimated that the free energy of reaction for bromellite + quartz = phenakite was between −14.31 and −6.48 kJ. This range agrees well with the value of −7.97 kJ (1000 K) calculated from the thermodynamic model. Bamberger and Baes used silica glass as the reference material for silica, and they were not able to achieve equilibrium in their beryllia-rich experiments. As a result their results are difficult to compare directly, but their calculated Gibbs free energy of formation is −1967.4 kJ, 61 kJ larger than the value derived here. The Bamberger and Baes value was not used in the evaluation, whereas the data of Schuiling and others were used.

Holm and Kleppa (1966) and Kiseleva and Shuriga (1981) measured the heats of solution of bromellite, phenakite, and quartz and derived enthalpies of reaction for bromellite + quartz = phenakite of −19.7(2.5) and −25.7(4.4) kJ at 968 K, respectively. The ΔH_{968} calculated in this study is −13.8 kJ, slightly greater than two standard deviations larger. Although there is no obvious reason for this discrepancy, the source probably lies in the solution calorimetry (O. J. Kleppa, pers. comm.). The more negative values of Holm and Kleppa (1966) and Kiseleva and Shuriga (1981) are not consistent with the occurrence of bromellite with talc in metasomatized ultramafic rocks (Klementyeva, 1969)—the calorimetric values predict that phenakite + periclase or brucite would be stable instead. The phenakite heat-of-solution measurements were not included in the final data reduction.

Calorimetric enthalpies for the reaction bromellite + corundum = chrysoberyl (Holm and Kleppa, 1966; Robie et al., 1978) used in the data reduction agree with the final value within two standard errors. This result is important in demonstrating the overall consistency of the thermodynamic model in that the Gibbs free energies of the beryllium phases are tied to that of corundum through both andalusite and chrysoberyl within experimental error.

Kiseleva et al. (1984) determined heats of formation for bertrandite, beryl, chrysoberyl, euclase, and phenakite by high-temperature oxide-melt solution calorimetry. Their enthalpies were not used in the PHAS20 fit because only derived parameters are given in their abstract. I. A. Kiseleva (pers. comm., 1984) indicated that their oxide data are consistent with those of Robie et al. (1978) permitting a comparison of their results to this study. $H^{\circ}_{f,298}{}^{\text{this study}} - H^{\circ}_{f,298}{}^{\text{Kiseleva}} = 16.7(13.4), 31.4(12.1), -6.5(3.8), 11.4(4.6)$, and 11.3(4.2) kJ/mol for, respectively, beryl, bertrandite, chrysoberyl, euclase, and phenakite, where the numbers in parentheses are one standard deviation reported by Kiseleva et al. (1984). If the uncertainties in Table 7 are included, then the two sets fall within about two standard deviations of each other. The differences are, however, still somewhat larger than expected, and full interpretation must await publication of the experimental results by Kiseleva and others.

The free energy of behoite was calculated from the average of the three heats of formation given by Stull and Prophet (1974) and the entropies from Robie et al. (1978) and Kostryukov et al. (1977).

The free energies and entropies estimated in this study are quite similar to those estimated in an earlier version (Barton, 1981). Only the entropy of euclase differs by an unexpectedly large amount, being 10 J/K·mol lower in this study. The difference in the estimated entropy for euclase leads to significant differences in the positions of some euclase-bearing equilibria.

Calculated mineral stabilities

The fitted thermodynamic properties can be used to calculate beryllium-mineral stabilities in the BASH system and, in conjunction with data from other sources, equilibria in more complex systems. In this section, several calculated phase diagrams are presented, discussed in terms of their agreement with natural assemblages, and compared with phase relations proposed for the BASH system by Burt (1978), Franz and Morteani (1981), and Hsu (1983). Figures 10, 11, and 12 show, respectively, pressure-temperature, log $a_{H_4SiO_4}$–temperature, and log $a_{Al_2O_3}$–temperature projections of the phase relations.

The overall pressure-temperature stabilities for the stoichiometric beryllium minerals are well defined (Fig. 10). With decreasing temperature, beryl + aluminum silicate replaces chrysoberyl + quartz under water-saturated conditions. In the 300–400°C range, beryl + aluminum silicate assemblages are replaced by euclase-containing assemblages. About 100° lower, pure beryl + water reacts to euclase- or bertrandite-bearing assemblages and phenakite + water goes to bertrandite. In general, the uncertainty in the reactions increases with decreasing temperature mainly because the hydration model is likely to be less adequate. A related problem is the increased uncertainty associated with extrapolation of the Gibbs free energies to temperatures lower than those of the experiments. Overall, ±30°C seems a conservative estimate of the uncertainty in the reactions that are not directly constrained by experiments. Because the uncertainties are highly correlated, the overall topology of the phase diagrams should not vary greatly.

Although the overall sequences and temperatures are well defined, some details of the topology remain uncertain. The uncertainties mainly involve reactions that mark the high-temperature limit of euclase + quartz. There are many possible configurations because the pertinent reactions involve the aluminum silicates and fall within the same range where aluminum silicate phase transitions oc-

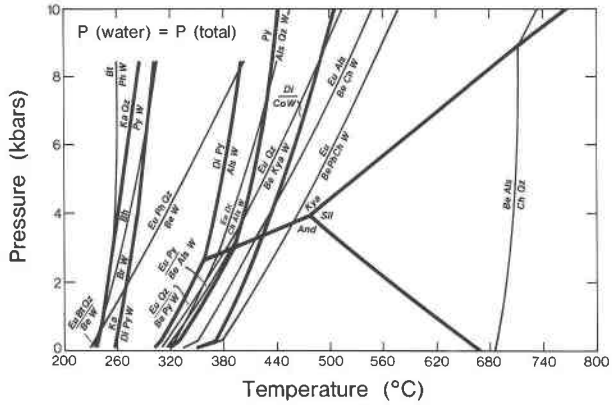

Fig. 10. Calculated water-saturated phase relations in the BeO-Al_2O_3-SiO_2-H_2O system. Abbreviations from Table 1.

cur. For example, the invariant point at about 3500 bars and 400°C among the phases beryl, euclase, kyanite, pyrophyllite, quartz, and water could be several kilobars higher in pressure or so much lower in pressure as to be metastable.

The log activity–temperature relations (Figs. 11, 12) present useful alternative projections of the BASH phase relations at 1 kbar. These are calculated from the thermodynamic model using the relation $\Delta G^{\circ}_{T,P} = -RT \ln a_i$, where a_i is the activity of the species of interest. The uncertainties in these diagrams are probably <0.15 log units.

Figure 12 is a nonconventional projection that deserves some comment. The activity of alumina is rarely considered an independent variable in petrology, perhaps because of the relative immobility of aluminum in most geologic environments. The activities of other components such as silica, the alkalis, alkaline earths, or hydrogen ion are used instead. Most complex equilibria involving aluminosilicate phases (feldspars, micas, chlorites, clays, etc.) can, however, be written with the activity of alumina as an independent variable. The advantage of doing this is that the stability limits of one set of minerals (in this case, beryllium minerals in the BASH system) can be shown with a wide variety of completely different reactions. For example, even though only the K-feldspar–muscovite buffer is shown on Figure 11, many other alumina buffers could be shown including serpentine-clinochlore-talc, albite-paragonite, topaz-quartz, and anorthite-zoisite-quartz, each of which is of interest in certain beryllium deposits.

Solid solution in beryl should have a substantial effect on the phase relations. Figures 11B and 12B show the calculated phase relations for the activity of beryl = 0.1. Activities of this magnitude are reasonable for natural alkali beryls assuming ideal mixing on the appropriate crystallographic sites. Alkali beryl commonly forms at late stages in pegmatite replacement zones replacing earlier, purer beryl and persisting to lower temperatures than would pure beryl (Beus, 1966).

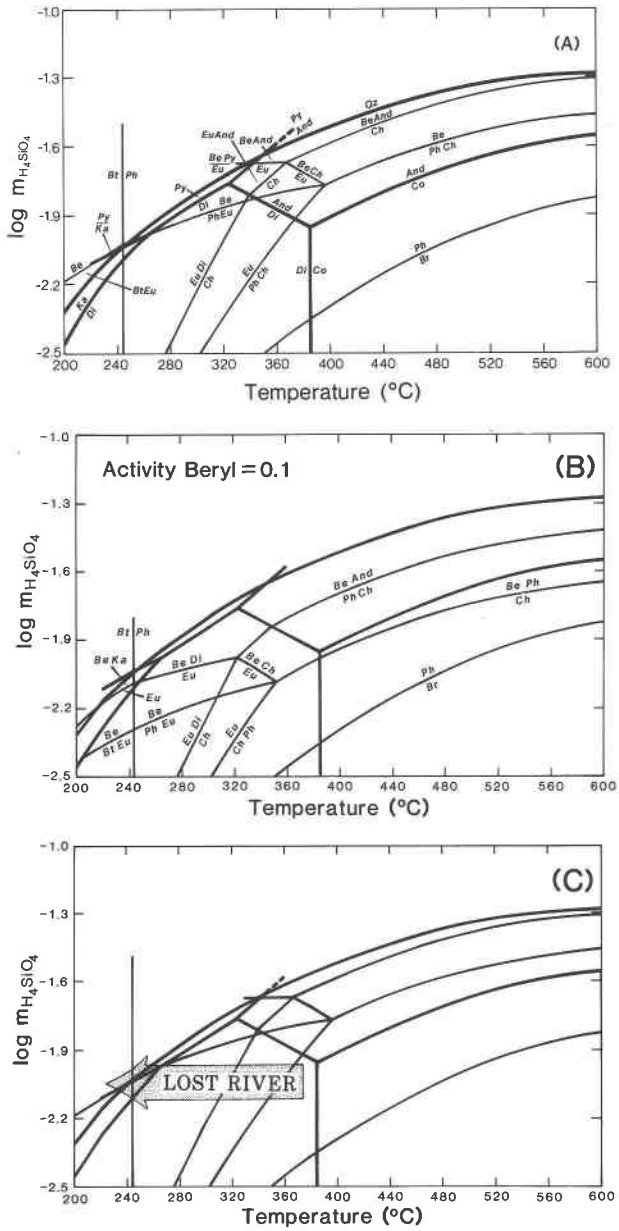

Fig. 11. Log $m_{H_4SiO_4}$–temperature projection of phase relations at 1 kbar. (A) Calculated phase relations for the pure system. (B) Calculated phase relations for $a_{beryl} = 0.1$. Note the large expansion of the beryl fields at the expense of the others. The curves are the same as in (A) except where labeled. (C) Path consistent with the sequence of assemblages seen in the Lost River, Alaska, beryllium deposits. The curves are the same as in (A). See text for discussion. Abbreviations from Table 1.

Compatibility with natural assemblages

A critical test of the calculated phase relations is how well they agree with observed beryllium-mineral parageneses. A large number of occurrences of two or three minerals in the BASH system have been described (see,

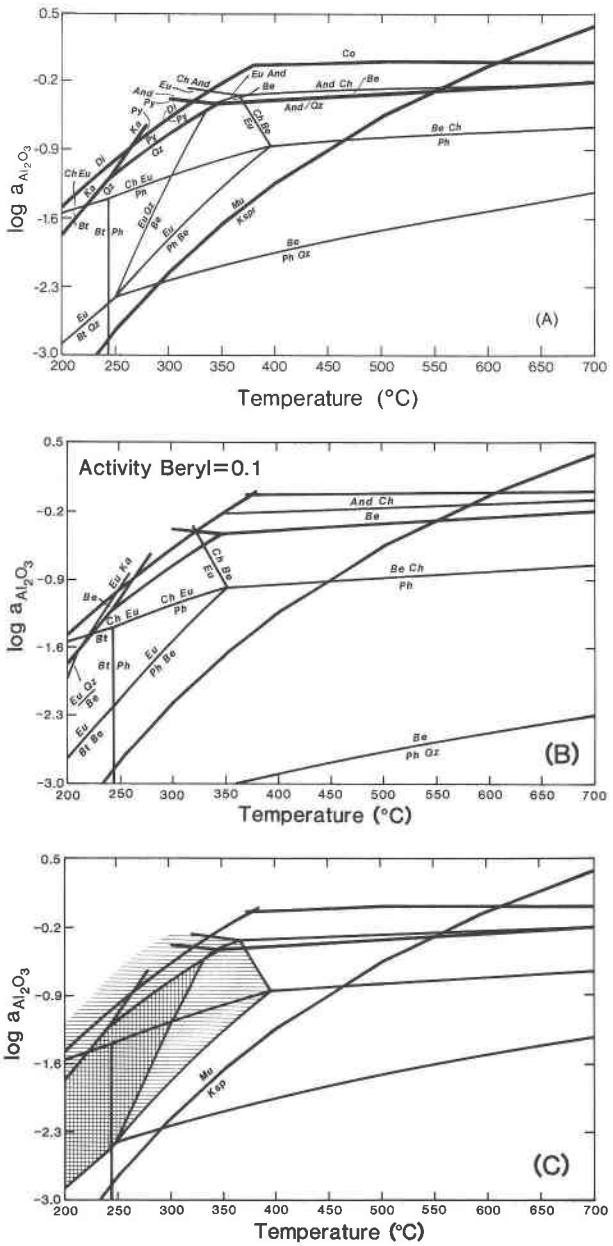

Fig. 12. Log $a_{Al_2O_3}$–temperature projection of BASH phase relations at 1 kbar. (A) Calculated phase relations for the pure system. Also shown is the curve for the reaction muscovite = K-feldspar + alumina + water. (B) Calculated phase relations for $a_{beryl} = 0.1$. The curves are the same as in (A) except where labeled. Note the effect of the expansion of the beryl stability fields. (C) Projection of the stability fields of euclase (horizontally ruled) and euclase + quartz (vertically ruled) with $a_{beryl} = 1$. The curves are the same as in (A). Note that euclase is incompatible with K-feldspar. See text for further discussion. Abbreviations from Table 1.

for example, Beus, 1966). Table 9 summarizes key, well-described associations of two or more minerals in the BASH system. The observed and calculated phase relations correspond well overall, but several associations have

Table 9. Proposed natural assemblages in the BeO-Al_2O_3-SiO_2-H_2O system

Assemblages	Occurrence	References
Ch + Ph + Be	pegmatites	Okrusch (1971)
Ch + Di	greisens, pegmatites	Sainsbury (1968), Appollonov (1967)
Ch + Qz + Sil	pegmatites	Heinrich and Buchi (1969), Stanek (1978), Franz and Morteani (1984)
Ch + Qz + Be	pegmatites	Heinrich and Buchi (1969)
Eu + Di (?)	greisens	Sainsbury (1968)
Co + Be	pegmatites	Graziani and Di Giulio (1979)
Ka + Be	greisens, pegmatites	Kayode (1971), Kerr (1946) Cerny (1968)
Ka + Be + Bt	pegmatites	Gallagher and Hawkes (1966)
Ka + Qz + Bt	volcanogenic deposits	Levinson (1962), Lindsey (1977)
Ka + Qz + Eu	greisens	Olsen (1971)
Be + Qz + Eu	pegmatites, greisens	Gallagher and Hawkes (1966), Kalyuzhnaya and Kalyuzhni (1963)
Be + Bt + Eu	pegmatites	Strand (1953), Komarova (1974)
Qz + Bt + Eu	pegmatites, greisens	Martenson (1960), Hawley (1969)
Qz + Bt + Be	pegmatites, greisens	many references
Qz + Ph + Be	pegmatites, greisens	Adams (1954), Kupriyanova (1970)
Be + Ph + Eu	pegmatites	Kalyuzhnaya and Kalyuzhni (1963)

small or nonexistent fields of stability, at least for activities of beryl near unity. These associations, discussed here, include corundum + beryl, kaolinite + beryl and/or + bertrandite, and beryl + bertrandite.

No pyrophyllite–beryllium-mineral assemblages have been described, which is unfortunate because pyrophyllite is a key phase in the predicted equilibria in the 300°C range. The activities of alkalis, alkaline earths, or fluorine are apparently high enough in the environments where the beryllium minerals form to replace pyrophyllite by micas, feldspars, or topaz.

Corundum + beryl. Corundum crystals have been reported as inclusions in a beryl crystal from Brazil (Graziani and Di Giulio, 1979). Because identification was made solely on the basis of electron microprobe analyses, which would not detect beryllium, and because some of the "corundum" was surrounded by quartz (Graziani and Guidi, 1979) it seems plausible that the mineral may be chrysoberyl. If it is corundum, then the association with quartz would indicate a disequilibrium assemblage. As can be seen from Figures 11A and 11B, only low activities of beryl (≤ 0.01) can be compatible with corundum.

Kaolinite + bertrandite. Kaolinite + bertrandite has been reported from volcanogenic beryllium deposits (Levinson, 1962; Lindsey, 1979). This assemblage is stable relative to euclase + quartz only at moderate pressures and low temperatures. Cogenetic silica in these deposits is represented by a poorly crystalline polymorph, indicating an unusually high silica activity at the time of formation. Hydrothermal K-feldspar is present with the kaolinite, also indicating metastability (with respect to muscovite). Silica activities much higher than quartz solubility are well known in geothermal waters and can significantly displace some equilibria such as the hydrolysis

of K-feldspar (Meyer and Hemley, 1967). The pertinent reaction here is $4BeAlSiO_4(OH) + 2SiO_2 + 3H_2O = Be_4Si_2O_7(OH)_2 + 2Al_2Si_2O_5(OH)_4$. Silica activities greater than that of quartz will drive the reaction to the right. Calculations based on the thermodynamic data indicate that a supersaturation of +0.6 (this study) or +0.2 (Hsu, 1983) log units will stabilize the right-hand side at 1 bar and 100°C. These concentrations are below that of amorphous silica at the same conditions, lending credence to the model. The abundant fluoride in these deposits may also help stabilize bertrandite (Hsu, 1983).

Bertrandite + beryl. Bertrandite very commonly replaces beryl, usually with a sheet silicate taking up the aluminum. The bertrandite + beryl assemblage, however, has only a small stability field in the simple system (Fig. 10). There are several possible explanations for this: a higher-temperature breakdown of bertrandite than proposed here; an underestimate of the stability of pure beryl at low temperatures; or the stabilization of beryl by solid solution. If the decomposition of bertrandite is close to the conditions indicated by Hsu (1983), the 100° increase over Figure 10 would dramatically broaden the field of coexistence of bertrandite and beryl. Two lines of evidence, however, support the lower-temperature breakdown proposed in this study. In an extensive fluid-inclusion study of bertrandite and phenakite from one deposit, Kosals et al. (1973) found that the bertrandite formed below 290°C and the phenakite above 200°C. Their estimate of the total pressure was 700 bars. Breakdown of bertrandite above 300°C would also preclude a stable field for the observed assemblage muscovite + phenakite + quartz (Franz et al., pers. comm.; Stager, 1960; cf. Fig. 12A).

As discussed above (Thermodynamics), the beryl hydration model is most likely to be inadequate at low temperatures and pressures leading to an underestimate of the stability of beryl. Thus it is possible that beryl + bertrandite could be much more extensive even with the lower-temperature bertrandite-breakdown reaction. Expansion of the beryl-stability field by solid solution, however, seems the most likely interpretation. Reasonable decreases in the activity of beryl greatly expand the beryl-stability field and hence the region of coexistence with bertrandite (Figs. 11, 12).

Kaolinite + beryl. Beryl most commonly alters to clays or micas plus other minerals. Černý (1968), Kayode (1971), and Kerr (1946) documented the alteration of beryl to kaolinite. The calculated phase relations indicate that this association is not stable at high activities of beryl (Figs. 11A, 12A), but that it does become stable with reasonable decreases in the activity of beryl (Figs. 11B, 12B). This interpretation is partly supported by the fact that the pegmatitic beryls discussed by Kerr (1946) and Černý (1968) tend to be alkali-rich and thus should have activities significantly less than 1. The association kaolinite + beryl + bertrandite (Gallagher and Hawkes, 1966) can be rationalized by silica supersaturation (Burt, 1978) only at low activities of beryl.

Comparison with alternative topologies

Burt (1978) proposed a detailed, general model for phase relations in the BASH system based on multisystems analysis and on the then-existing phase-equilibrium, mineral-association, and mineral-volume data. Although there are similarities between Burt's topology and the one calculated here, they differ substantially. The principal differences arise from two sources: interpretations of the P-T extent of the assemblage chrysoberyl + quartz and of the P-T extent of euclase stability at low temperatures. In the absence of reported natural assemblages of beryl with pyrophyllite or aluminum silicate, Burt omitted them from his multisystem. This omission led to the erroneous conclusion that chrysoberyl + quartz is stable to temperatures below the stability limits of the anhydrous aluminum silicates plus water; thus, the replacement of chrysoberyl in quartz-containing systems would be by a reaction such as chrysoberyl + quartz = beryl + kaolinite. In contrast, the experimental results on this reaction (Fig. 3) indicate that chrysoberyl + quartz breaks down to give beryl + aluminum silicate at temperatures substantially above the stability of kaolinite and pyrophyllite and probably above the stability limit of euclase.

As noted above, pyrophyllite—a key mineral in the calculated phase relations—has not been reported with beryllium minerals. The association chrysoberyl + euclase + quartz would support Burt's model, as would any hydrous aluminum silicate + chrysoberyl + quartz, but such assemblages have not been reported. In contrast, the association beryl + andalusite or sillimanite has been reported from several places, although the two always seem to be in a reaction relationship (Heinrich and Buchi, 1969; Franz and Morteani, 1984).

The paucity of the lower-temperature coexisting pairs beryl plus andalusite or sillimanite, which might be used to argue for their incompatibility, can be explained by a bulk-composition effect. Because pegmatites generally have abundant K-feldspar, aluminum silicate assemblages would not be expected in pegmatites for temperatures less than those of the reaction $KAl_2[AlSi_3O_{10}](OH)_2 + SiO_2 = KAlSi_3O_8 + Al_2SiO_5 + H_2O$. At higher pressures, this reaction is replaced by melting reactions (e.g., Huang and Wyllie, 1974). Franz and Morteani (1984) have proposed the formation of chrysoberyl + quartz by related melting reactions. Other evidence given by Franz and Morteani (1984) and Heinrich and Buchi (1969) suggests that chrysoberyl forms during a high-grade, probably prograde event. Chrysoberyl + quartz assemblages are not associated with later hydrous alteration even though they may contain crystals of substantial size. This suggests formation from high-temperature fluids such as melts. Chrysoberyl + quartz has been described by Franz and Morteani (1981) as reacting to beryl + muscovite. Although this is not within the BASH system, it does indicate that chrysoberyl + quartz is not highly stable as indicated by the narrowness of the muscovite + quartz field at high temperatures (Fig. 12).

Many alternative assemblages to chrysoberyl + quartz are known. An important possibility is euclase + diaspore. Sainsbury (1968) described euclase + white mica veinlets cutting diaspore + chrysoberyl replacement zones at Lost River, Alaska. It is possible, but not clear from his descriptions, that euclase may also coexist with diaspore. This association supports the thermodynamic model that predicts a broad stability range for this pair (Fig. 11) precluding the assemblage chrysoberyl + quartz at intermediate temperatures. Other reported associations, however, do not prohibit chrysoberyl + quartz at least at the higher temperatures. The apparent lack of appropriate natural bulk compositions precludes an unambiguous answer to this question.

The other significant distinction between Burt's topology and that calculated here is in his inference of the low-temperature breakdown of euclase to bertrandite + kaolinite assemblages. The thermodynamic model, however, suggests that bertrandite and kaolinite can coexist only under conditions of unusually high silica activity, consistent with the natural occurrences.

Hsu (1983) reproduced a portion of Burt's topology and indicated where the reactions that he determined fit in; however, neither his experimental data nor any others are compatible with the stable existence of the invariant point [Qz] shown in Hsu's Figure 6.

The BASH phase relations proposed by Franz and Morteani (1981) on the basis of their experimental results share some features with Figure 10 at intermediate and high temperatures. The similarity results from the large stability field for beryl + aluminum silicates (both hydrous and anhydrous) shown by Franz and Morteani in contrast to Burt (1978). There are, however, many differences in the details of the topology that result from the use by Franz and Morteani of Chatterjee's (1976) phase relations for the ASH system.

Franz and Morteani infer phase relations at lower temperatures by extrapolation of new reactions that result from the intersection of their experimentally determined reactions. These extrapolations indicate a minimum pressure for euclase + quartz of about 2 kbar and lead to a low-temperature topology similar to that of Burt (1978). Such graphical extrapolations are uncertain, and the predictions conflict with the thermodynamic extrapolations done in this study on the basis of a similar, but far more extensive set of experimental results.

Phase equilibria in more complex systems

Most beryllium minerals occur in rocks with more components than those in the BASH system. The most important of these additional components are the Na_2O, K_2O, and CaO that form feldspars, micas, and clays. Feldspar-mica equilibria are represented in Figure 12 by the reaction $KAlSi_3O_8 + H_2O + (Al_2O_3) = KAl_2[AlSi_3O_{10}](OH)_2$, where alumina is enclosed in parentheses to emphasize that in general it is not represented by corundum. Other components important in equilibria involving beryllium-aluminum silicates include Li, Mg, Mn, Fe, Zn, P, S, and F. Additional feldspar-mica and many other reactions could be calculated using a suitable data base (e.g., Robie et al., 1978). The topologies of the phase relations in more complex systems have been discussed by many authors, notably Burt (1975a, 1975b, 1980), Kupriyanova (1982), and Beus and Dikov (1967).

Some petrologic applications

A comprehensive discussion of the parageneses of beryllium minerals in this system and related, more complex systems is beyond the scope of this study. Instead, some general observations on the parageneses of beryllium minerals will be presented in terms of the predictions of the thermodynamic model. The calculated phase relations constrain not only the pressures and temperatures of formation of beryllium-mineral assemblages, but they also place useful constraints on the activities of silica and alumina. With few exceptions, discrete beryllium minerals are found only in alkalic felsic igneous rocks and related metasomatic rocks. The distribution of beryllium minerals is thoroughly discussed by Vlasov (1967, Vols. II and III) and Beus (1966) and will not be reviewed here.

Limitations on pressure and temperature

The variation in beryllium mineral assemblages from pegmatites to greisens to volcanogenic deposits (Table 9) is consistent with a trend of generally decreasing pressure and temperature. The calculated phase relations in the quaternary system agree with observed assemblages as discussed in the last section. The paucity of uniquely high- or low-pressure assemblages precludes the estimation of pressure. The phase relations provide reasonable temperature constraints, although solid solution in beryl should cause large changes in the positions of beryl-bearing equilibria.

Only euclase + phenakite + quartz or beryllium minerals with kyanite have nontrivial minimum pressures of formation (ca. 0.5 and 2.5 kbar, respectively, but highly uncertain for the former). Neither of these assemblages has been reported. The fields of the low-pressure assemblages bertrandite + beryl, pyrophyllite + beryl, and andalusite + other phases are similarly uncertain.

BASH phase equilibria provide useful temperature constraints. The assemblage chrysoberyl + quartz indicates amphibolite- to granulite-grade conditions, except under conditions of reduced volatile pressure. Euclase- and bertrandite-bearing assemblages restrict maximum temperatures to middle and lower greenschist facies, respectively. More precise estimates might be made for particular assemblages, if solid solution in beryl is accounted for. Because most beryllium minerals form in dynamic environments where temperatures and possibly pressures change substantially during petrogenesis, the sequence of assemblages and hence the T(-P) paths are generally of greater interest than specific temperature or pressure estimates. For example, consider the formation of pegmatites. The small size of pegmatites requires that they cool quickly to

the temperature of their surroundings, but subsequently their conditions change quite slowly along with the host rocks. If the pegmatitic fluids are lost fairly rapidly, the fluid-dominated crystallization processes will reflect temperatures only down to that of the host at the time of formation. Therefore, the beryllium minerals (and many others) might be used to constrain the cooling path and place an upper bound on the temperature of the host rocks at the time of emplacement.

Equilibria in more complex systems have not been calculated here with the exception of the K-feldspar–muscovite reaction in Figure 12. Franz et al. (unpub. ms.) discussed the formation of beryl from phenakite in Alpine prograde regional metamorphism by several reactions, among them $2KAl_2[AlSi_3O_{10}](OH)_2 + 3Be_2SiO_4 + 9SiO_2 = 2Be_3Al_2Si_6O_{18} + 2KAlSi_3O_8 + 2H_2O$. At 6 kbar, this reaction should take place at about 420°C, which is 80–130° below the peak temperatures estimated from other reactions in the same rocks (Franz et al., unpublished manuscript), but consistent with the mineral associations in pegmatites where beryl + K-feldspar is much more common than phenakite + muscovite.

Limitations on activities of components

In most occurrences, textural evidence suggests that only a single beryllium mineral is stable in a given assemblage. If more than one is present, textures commonly indicate a reaction relation. As a component present in but one phase in a given assemblage, BeO could be ignored in the consideration of equilibria in a rock, much as other trace components can be neglected (e.g., Miyashiro, 1975, p. 125). A trace component (such as zirconia) that is almost always present in the same mineral (zircon, in granites) has a limited utility as an indicator of the intensive variables (e.g., *T, P,* chemical potentials) during petrogenesis. In contrast, the several minerals in the BASH system, which share all but one component with major phases, yield constraints on the activities of the major components (Al_2O_3, SiO_2, and H_2O). This is particularly important in metasomatic rocks where there are many degrees of freedom and where estimates of activities are needed in order to make petrogenetic interpretations. Comparison of the total set of buffers to the beryllium-free buffers in Figures 11 and 12 illustrates the superior resolution possible with beryllium minerals present. This use of the beryllium minerals in metasomatic rocks is analogous to the evaluation of the activities of major components in igneous rocks (e.g., Carmichael et al., 1974).

The activity of water is the most difficult of the three to evaluate directly. Only chrysoberyl + quartz can be easily interpreted with water pressure as an independent variable; however, because other volatiles should stabilize beryl in the same way that water does, there will still be ambiguities in interpretation.

Log $a_{H_4SiO_4}$. Beryllium minerals are good indicators of silica activities (Fig. 11) and hence can be used to interpret the conditions and processes of formation. Beryllium-mineral parageneses in "apocarbonate" greisens and "crossing-line" (desilicated) pegmatites (Vlasov, 1967, Vol. III) offer excellent examples. Apocarbonate greisens form by addition of fluorine, alumina, alkalis, silica, and trace elements from granites to nearby carbonate rocks. In the Lost River, Alaska, beryllium deposits described by Sainsbury (1968), the earliest mineralization is replacement of limestone by fine-grained diaspore, fluorite, and "curdy" chrysoberyl. This stage is cut by euclase-(bertrandite-)mica-fluorite veins that are in turn followed by muscovite-fluorite-beryl-quartz veins. This sequence can be simply interpreted as the consequence of the cooling and progressive reaction of fluids derived from associated greisenized granite. Figure 11C shows this path superimposed on the 1-kbar aqueous-silica phase relations. The Lost River assemblages are consistent with a path across the diagram from high to low temperature and from low to high silica activities (the activity of quartz is unity on the quartz saturation line). At the highest temperatures and low silica activities, chrysoberyl + diaspore is stable; with decreasing temperature, chrysoberyl should react to give euclase and diaspore. Further decrease in temperature results in the decomposition of euclase to give pyrophyllite + beryl and eventually to precipitation of quartz. Alkalies in the fluids at Lost River were apparently concentrated enough to give micas in place of the pure aluminous phases at lower temperatures. The large undersaturation in silica is likely due to the retrograde solubility of quartz at the moderate temperatures and low pressures of formation of the deposit (Dobson, 1982; Walther and Helgeson, 1977). This would cause initially quartz-saturated fluids coming from the granite to go through a quartz-undersaturated region leading to silica-deficient assemblages. Progressive cooling would lead to the restoration of a prograde silica solubility and eventually a concomitant increase in the silica content of the precipitated minerals.

At higher pressures, the solubility of quartz is prograde at all temperatures. Therefore, similar apocarbonate greisens formed at higher pressures should show more silicious assemblages. This appears to be the case at McCullough Butte, Eureka County, Nevada, where beryl and late bertrandite are the predominant beryllium minerals (Barton, 1982a). At McCullough Butte, the vein assemblages are mostly quartz-saturated with the exception of a quartz-free muscovite-dominated association that in turn is followed by quartz-rich muscovite-fluorite veins.

Crossing-line (desilicated) pegmatites commonly show zoning from beryl (± quartz) in the centers to chrysoberyl and/or phenakite in outer (silica-poor) parts (Beus, 1966; Vlasov, 1967). This sequence is compatible with a path from high to low silica activities at relatively high temperatures (Fig. 11). In a few localities where beryllium-rich solutions reacted with ultramafic rocks, the silica activity was reduced beneath the phenakite-bromellite reaction producing bromellite (in highly magnesian assemblages, Klementyeva, 1969; Smirnov, 1977). At constant temperature, the presence of talc + antigorite buffers aqueous silica just below the value for bromellite + phen-

akite (Fig. 6, Hemley et al., 1977b) consistent with the occurrence of bromellite with talc (Klementyeva, 1969).

Log $a_{Al_2O_3}$. Beryllium-mineral parageneses can also provide useful constraints on the activity of alumina. As discussed above, alumina is generally a fixed component, that is, other components (alkalies, hydrogen ion, silica, and halogens) are generally more mobile and thus used in conventional projections of the phase equilibria. The advantage, however, of treating the activity of alumina as an independent variable is that it allows direct comparison of a variety of beryllium-mineral equilibria on the same diagram without having to draw a separate diagram for each new set of additional components. For example, the activity of alumina is related to conventional hydrolysis reactions (and hence hydrogen ion and alkali concentrations) by reactions such as the following:

$$KAlSi_3O_8 + H_2O + (Al_2O_3) = KAl_2[AlSi_3O_{10}](OH)_2 \quad (11a)$$

$$3KAlSi_3O_8 + 2H^+ = 2K^+ + 6SiO_2 + KAl_2[AlSi_3O_{10}](OH)_2 \quad (11b)$$

$$2KAlSi_3O_8 + 2H^+ = 2K^+ + H_2O + 6SiO_2 + (Al_2O_3). \quad (11c)$$

As can be seen from Reaction 11c, which is the difference of 11a and 11b, the activity of alumina is inversely related to $(a_{K^+})^2$ and proportional to $(a_{H^+})^2$. Similar relationships exist for other hydrolysis reactions as well as for many other kinds of reactions (e.g., fluorination reactions).

An immediate consequence of examining such a diagram is an explanation for the comparative rarity of euclase in spite of the central role that it plays in the calculated phase equilibria in the BASH system. There are two related reasons for its rarity. First, as can be seen in Figure 12C, euclase and quartz are stable together only at relatively low temperatures. Because most beryllium-rich assemblages are quartz saturated (most pegmatites and greisens), the quartz + euclase reaction represents the most common upper limit. Still, euclase + quartz is stable to higher temperatures than bertrandite, yet bertrandite is much more common. The second reason for the rarity of euclase is made clear by Figure 12. Euclase requires a relatively high chemical potential of alumina, above that at which K-feldspar is stable. In many greisens and nearly all pegmatites the alumina contents are buffered by reactions such as 11 between the white micas, feldspars, topaz, and quartz. Muscovite, K-feldspar, and quartz fix the chemical potential of alumina in the beryl field over most of the temperature range (Fig. 12). Topaz-quartz (-muscovite) assemblages which begin at the andalusite-quartz line and extend downward do likewise, although at high fluorine fugacities, they may buffer $\mu_{Al_2O_3}$ to values within the quartz + phenakite field. The reaction $2Be_3Al_2Si_6O_{18} + 4HF = 3Be_2SiO_4 + 2Al_2SiO_4F_2 + 7SiO_2 + 2H_2O$ has been proposed by Burt (1975b) as a natural fluorine buffer; such assemblages, while uncommon, are known in pegmatites, miarolitic cavities, and some greisens (Barton, 1982b). These relationships explain why euclase is usually found in rocks deficient in the alkalies relative to alumina, such as hydrolytically altered rocks (e.g., aluminosilicate greisens). Although expansion of the stability field of beryl with solid solution may also play a role in diminishing the stability field of euclase, the high H^+ to total alkali ratio (Reaction 11c) would work against this. Consistent with this, most greisen beryls are more nearly stoichiometric than late-stage pegmatitic beryls that formed at similar temperatures (Beus, 1966).

The topology of Figure 12 illustrates the reason that muscovite + bertrandite + quartz is the most common assemblage to replace beryl. Beryl + K-feldspar cooling with fluid will react accordingly to give muscovite + phenakite or bertrandite at temperatures below 250°C at 1 kbar. Because the interval for phenakite is quite small, the predominant product will be bertrandite. In fact, the only product will be bertrandite if the stability field of beryl is expanded slightly by solid solution.

Because the chemical potentials of the alkalis vary inversely with that of alumina in quartz + mica or feldspar assemblages, the variations described here may equally well be thought of as due to variations in alkalinity (with alumina as an inert component). The absence of chrysoberyl and the relative abundance of bertrandite, phenakite, and the alkali-beryllium silicates in peralkaline granites and syenites (cf., Beus, 1966; Vlasov, 1967, Vol. II) reflect the low intrinsic chemical potentials of alumina in these rocks. In peralkaline rocks, alumina-undersaturated minerals such as acmite and riebeckite require that the alumina activities be significantly below that of the K-feldspar–muscovite buffer (Reaction 11). Alumina-buffering reactions involving peralkaline minerals will be below the stability fields of euclase and chrysoberyl and, especially in the absence of quartz, will be below the stability field of beryl, thus rationalizing the observed abundance of the aluminum-free beryllium silicates in peralkaline rocks.

Summary

The thermodynamic properties of behoite, bertrandite, beryl, chrysoberyl, euclase, and phenakite have been evaluated from a combination of new phase-equilibrium, calorimetric, and volumetric measurements along with data from the literature. Of 86 data sets containing over 1000 observations, only one set does not fit the model or have good reasons for being discarded. The resulting internally consistent thermodynamic model is compatible with natural assemblages in the BASH system and provides a suitable basis for the prediction of equilibria in more complex systems.

Beryllium minerals in the BASH system provide limits on the temperatures and activities of silica and alumina during formation. Beryl has a broad stability range, consistent with its natural abundance. The stability of beryl is significantly enhanced by incorporation of volatile species and alkalis. The effect of volatile incorporation is

modeled as a simple volumetric interaction. This model works well for beryl and appears reasonable for cordierite, although it results in a somewhat poorer fit than the other, more elaborate models proposed for cordierite. Solution of nonvolatile species in beryl is also inferred to have a major effect on equilibria involving beryl.

Occurrences of the BASH minerals provide broad constraints on temperature, but no independent pressure constraints. Chrysoberyl + quartz is restricted to high temperatures except when $P_{fluid} < P_{total}$. Euclase-bearing assemblages replace aluminous beryl-bearing assemblages in the 300–500°C range. Stoichiometric beryl breaks down in the presence of water about 100°C lower, although alkali-rich beryls will persist to lower temperatures. The results of this study indicate that bertrandite and behoite are stable only below 260°C in agreement with the limited natural data, although the results of Hsu (1983) suggest that bertrandite is stable to 350°C.

Because beryllium minerals most commonly occur singly in metasomatic rocks, perhaps their most useful petrologic attribute is as indicators of the activities of silica and alumina. For example, the beryllium minerals permit a much finer discrimination of the activities of silica in apocarbonate greisens and desilicated pegmatites than would be possible from the phases of the major elements alone. Similarly, the beryllium minerals provide additional constraints on the activities of alumina in greisens. Euclase, for example, is stable only at elevated alumina activities, indicating environments where the alkalis have unusually low activities either as a consequence of acid metasomatism (as in aluminosilicate greisens), or unusually low initial alkali contents and high aluminum mobility (as in apocarbonate greisens).

Additional studies that might help resolve problems found here are an improved determination of Reaction 4, more data on equilibria below 400°C (solubility experiments might work best), direct beryl hydration measurements, evaluation of the effect of solid solution on beryl stability (perhaps by displacement of Reaction 1), and investigation of the occurrence of critical natural assemblages such as chrysoberyl + quartz + euclase or euclase + andalusite.

Acknowledgments

It is a pleasure to acknowledge helpful reviews by D. M. Burt, W. A. Dollase, W. G. Ernst, and R. C. Ewing on this paper, and by J. R. Goldsmith, P. B. Moore, R. C. Newton, and P. J. Wyllie on an earlier version. Many other people contributed helpful discussions or assistance on various aspects of this project including P. B. Barton, Jr., J. L. Haas, Jr., H. T. Haselton, J. J. Hemley, D. M. Jenkins, W. Moloznik, D. Perkins III, G. R. Robinson, Jr., P. Toulmin III, and W. J. Ullman. R. C. Aller provided the facilities for and help with the silica analyses. The experimental work was supported by NSF grant EAR78-13675 to J. R. Goldsmith. Support for the thermodynamic modeling was obtained from EAR84-08388 to M. D. Barton. While a student, I was supported by a National Science Foundation Graduate Fellowship and by a McCormick Fellowship from the University of Chicago.

References

Adams, J.W. (1953) Beryllium deposits of the Mount Antero region, Chaffee County, Colorado. U.S. Geological Survey Bulletin 982-D, 95–119.

Aines, R.D.F., and Rossman, G.R. (1984) The high temperature behavior of water and carbon dioxide in cordierite and beryl. American Mineralogist, 69, 319–327.

Appolonov, V.N. (1967) Morphological feature of chrysoberyl from Sargodon. Zapiski Vsesoyunogo Mineralogichekogo Obshchestva, 96, 329–332.

Bamberger, C.E., and Baes, C.F., Jr. (1972) Equilibria of SiF_4 with SiO_2, Be_2SiO_4, and BeO in molten Li_2BeF_4. American Ceramic Society Journal, 55, 564–568.

Barton, M.D. (1981) The thermodynamic properties of topaz and some minerals in the system BeO-Al_2O_3-SiO_2-H_2O. Ph.D. thesis, University of Chicago, Chicago, Illinois.

——— (1982a) Some aspects of the geology and mineralogy of the fluorine-rich skarn at McCullough Butte, Eureka County, Nevada. Carnegie Institution of Washington Year Book 81, 324–328.

——— (1982b) The thermodynamic properties of topaz solid solutions and some petrologic applications. American Mineralogist, 67, 956–974.

Beus, A.A. (1966) Geochemistry of beryllium and genetic types of beryllium deposits. W. H. Freeman and Company, San Francisco.

Beus, A.A., and Dikov, Yu. P. (1967) The geochemistry of beryllium in the processes of endogenetic mineralization. Nedra, Moscow.

Bukin, G.V. (1967) Crystallization conditions of the phenakite-bertrandite-quartz association (experimental data). Akademiya Nauk SSSR Doklady, 176, 664–667.

Burnham, C.W. (1962) Lattice constant refinement. Carnegie Institution of Washington Year Book 61, 132–135.

Burt, D.M. (1975a) Beryllium mineral stabilities in CaO-BeO-SiO_2-P_2O_5-F_2O_{-1} and the breakdown of beryl. Economic Geology, 70, 1279–1292.

——— (1975b) Natural fluorine buffers in the system BeO-Al_2O_3-SiO_2-F_2O_{-1}. (abs.) EOS American Geophysical Union Transactions, 56, 467.

——— (1976) Generation of high HF fugacities in miarolitic pegmatites and granites: The possible role of topaz. Geological Society of America Abstracts with Programs, 8, 798.

——— (1978) Multisystems analysis of beryllium mineral stabilities: The system BeO-Al_2O_3-SiO_2-H_2O. American Mineralogist, 63, 664–676.

——— (1980) The stability of danalite, $Fe_4Be_3(SiO_4)_3S$. American Mineralogist, 65, 355–361.

——— (1982) Minerals of beryllium. In P. Černý, Ed., Granitic pegmatites in science and industry, 135–148. Mineralogical Association of Canada Short Course Handbook 8.

Carmichael, I.S.E., Turner, F.J., and Verhoogen, J. (1974) Igneous petrology. McGraw-Hill, New York.

Černý, P. (1968) Beryllumwandlungen in Pegmatiten-Verlauf und Produkte. Neues Jahrbuch für Mineralogie Abhandlungen, 108, 166–180.

——— (1975) Alkali variations in pegmatitic beryl and their petrogenetic implications. Neues Jahrbuch für Mineralogie Abhandlungen, 123, 198–212.

Chatterjee, N.D. (1976) Margarite stability and compatibility relations in the system CaO-Al_2O_3-SiO_2-H_2O as a pressure-temperature indicator. American Mineralogist, 61, 699–709.

Cline, C.F., Morris, R.C., Dutoit, M., and Harget, P.J. (1979) Physical properties of $BeAl_2O_4$ single crystals. Materials Science Journal, 14, 941–944.

Cohen, J.P., Ross, F.K., and Gibbs, G.V. (1977) An X-ray and neutron diffraction study of hydrous low cordierite. American Mineralogist, 62, 67–78.

Demarest, H.H., Jr., and Haselton, H.T. (1981) Error analysis

for bracketed phase equilibrium data. Geochimica et Cosmochimica Acta, 45, 217–224.

Ditmars, D.A., and Douglas, T.B. (1967) Relative enthalpy of beryllium 1:1 aluminate, $BeO \cdot Al_2O_3$ from 298 to 1173 K. Thermodynamic properties from 273 to 2150 K. National Bureau of Standards Journal of Research, 71A, 89–95.

Dobson, D.C. (1982) Geology and alteration of the Lost River tin-tungsten-fluorine deposit, Alaska. Economic Geology, 77, 1033–1052.

Fleischer, M. (1980) Glossary of mineral species 1980. Mineralogical Record, Tucson, Arizona.

Frantz, J.D., and Hare, P.E. (1973) The analysis of silica at submicrogram levels using a flow-cell colorimetric technique. Carnegie Institution of Washington Year Book 72, 704–706.

Franz, G., and Morteani, G. (1981) The system BeO-Al_2O_3-SiO_2-H_2O: Hydrothermal investigation of the stability of beryl and euclase in the range from 1 to 6 kb and 400 to 800°C. Neues Jahrbuch für Mineralogie Abhandlungen, 140, 273–299.

——— (1984) The formation of chrysoberyl in metamorphosed pegmatites. Journal of Petrology, 25, 27–52.

Furukawa, G.T., and Saba, W.G. (1966) Heat capacity and thermodynamic properties of beryllium aluminate (chrysoberyl), $BeO \cdot Al_2O_3$, from 16 to 380K. National Bureau of Standards Journal of Research, 69A, 13–18.

Gallagher, M.J., and Hawkes, J.R. (1966) Beryllium minerals from Rhodesia and Uganda. Geological Survey of Great Britain Bulletin, 25, 59–75.

Ganguli, D. (1972) Crystallization of beryl from solid-solid reactions under atmospheric pressure. Neues Jahrbuch für Mineralogie Monatshefte, 1972, 193–199.

Ganguli, D., and Saha, P. (1967) A reconnaissance of the system BeO-Al_2O_3-SiO_2-H_2O. Indian Ceramic Society Transactions, 26, 102–110.

Gibbs, G.V., Breck, D.W., and Meagher, E.P. (1968) Structural refinement of hydrous and anhydrous synthetic beryl, $Al_2(Be_3Si_6O_{18})$ and emerald, $Al_{1.9}Cr_{0.1}(Be_3Si_6O_{18})$. Lithos, 1, 275–285.

Ginzburg, A.I. (1955) Chemical composition of beryl. Trudy Mineralogichekogo Muzeya Akademiya Nauk SSSR, 7 (not seen; cited in Beus, 1966).

Goldman, D.S., Rossman, G.R., and Dollase, W.A. (1977) Channel constituents in cordierite. American Mineralogist, 62, 1144–1157.

Goldman, D.S., Rossman, G.R., and Parkin, K.M. (1978) Channel constituents in beryl. Physics and Chemistry of Minerals, 3, 225–237.

Graziani, G., and Di Giulio, V. (1979) Growth of an aquamarine crystal from Brazil. Neues Jahrbuch für Mineralogie Monatshefte, 1979, 101–108.

Graziani, G., and Guidi, G. (1979) Mineralogical study of a starberyl and its inclusions. Neues Jahrbuch für Mineralogie Monatshefte, 1979, 86–92.

Haar, L., Gallagher, J., and Kell, J.S. (1979) Thermodynamic properties for fluid water. Water and steam—Their properties and current industrial applications. Proceedings of the 9th International Conference on the Properties of Steam, 69–82.

——— (1981) The anatomy of the thermodynamic surface of water: The formulation and comparisons with data. Proceedings of the 8th Symposium on Thermophysical Properties, 298.

Haas, J.L., Jr., and Fisher, J.R. (1976) Simultaneous evaluation and correlation of thermodynamic data. American Journal of Science, 276, 525–545.

Haas, J.L., Hemingway, B.S., and Robinson, G.L., Jr. (1980) Tables for the thermodynamic properties of phases in the CaO-Al_2O_3-SiO_2-H_2O. U.S. Geological Survey Open-File Report 80–908.

Halbach, H., and Chatterjee, N.D. (1984) An internally consistent set of thermodynamic data for twenty-one CaO-Al_2O_3-SiO_2-H_2O phases by linear parametric programming. Contributions to Mineralogy and Petrology, 88, 14–23.

Hawthorne, F.C., and Černý, P. (1977) The alkali-metal positions in Cs-Li beryl. Canadian Mineralogist, 15, 414–421.

Hazen, R.M., Finger, L.W., and Barton, M.D. (1983) High-pressure structures and compressibilities of bertrandite, beryl, and euclase. Carnegie Institution of Washington Year Book 82, 361–363.

Heinrich, E.W., and Buchi, S.H. (1969) Beryl-chrysoberyl-sillimanite paragenesis in pegmatites. Indian Mineralogist, 10, 1–7.

Helgeson, H.C., Delany, J.H., Nesbitt, H.W., and Bird, D.K. (1978) Summary and critique of the thermodynamic properties of rock-forming minerals. American Journal of Science, 278-A.

Hemingway, B.S., Barton, M.D., Robie, R.A., and Haselton, H.T., Jr. (1986) The heat capacities and thermodynamic functions for beryl, $Be_3Al_2Si_6O_{18}$, phenakite, Be_2SiO_4, euclase, $BeAlSiO_4(OH)$, bertrandite, $Be_4Si_2O_7(OH)_2$, and chrysoberyl, $BeAl_2O_4$. American Mineralogist, 71, 557–568.

Hemley, J.J., Montoya, J.W., Christ, C.L., and Hostetler, P.B. (1977a) Mineral equilibria in the system MgO-SiO_2-H_2O: I. Talc-chrysotile-forsterite-brucite-stability relations. American Journal of Science, 277, 322–351.

Hemley, J.J., Montoya, J.W., Shaw, D.R., and Luce, R.W. (1977b) Mineral equilibria in the MgO-SiO_2-H_2O system: II. Talc-antigorite-forsterite-anthopyllite-enstatite stability relations and some geologic implications in the system. American Journal of Science, 277, 353–383.

Hemley, J.J., Montoya, J.W., Marinenko, J.W., and Luce, R.W. (1980) Equilibria in the system Al_2O_3-SiO_2-H_2O and some general implications for alteration/mineralization processes. Economic Geology, 75, 210–228.

Holland, T.J.B. (1980) The reaction albite = jadeite + quartz determined experimentally in the range 600–1200°C. American Mineralogist, 65, 129–134.

Holm, J. L., and Kleppa, O.J. (1966) High-temperature calorimetry in liquid oxide systems. Acta Chemica Scandinavica, 20, 2568–2572.

Hsu, L.C. (1983) Some phase relationships in the system BeO-Al_2O_3-SiO_2-H_2O with comments on the effect of HF. Geological Society of China Memoir 5, 33–46.

Huang, W.L., and Wyllie, P.J. (1974) Melting relations of muscovite with quartz and sanidine in the K_2O-Al_2O_3-SiO_2-H_2O system to 30 kilobars and an outline of paragonite melting relations. American Journal of Science, 274, 378–395.

Jochum, C., Mirwald, P.W., Maresch, W., and Schreyer, W. (1983) The kinetics of H_2O exchange between cordierite and fluid during retrogression. Fortschritte der Mineralogie, 61, 103–105.

Johannes, W., and Schreyer, W. (1981) Experimental introduction of CO_2 and H_2O into Mg-cordierite. American Journal of Science, 281, 299–317.

Kalyuzhnaya, K.M., and Kalyuzhnyi, V.A. (1963) The paragenesis of accessory beryl, phenakite, and euclase in topaz-morion (smoky quartz) pegmatites. Mineralogichekogo Sbornik (L'vov), 17, 135–147.

Kayode, A.A. (1971) A kaolinite greisen from Dorowa-Babuje, northern Nigeria. Economic Geology, 66, 811–812.

Kelley, K.K. (1939) The low temperature heat capacities of BeO (bromellite) and Be_2SiO_4 (phenacite). American Ceramic Society Journal, 61, 1217–1219.

Kerr, P.F. (1946) Kaolinite after beryl from Alto do Giz, Brazil. American Mineralogist, 31, 435–442.

Kiseleva, I.A., and Shuriga, T.N. (1981) New data on the thermodynamic properties of phenakite. Akademiya Nauk SSSR Doklady, 266, 310–313.

Kiseleva, I.A., Ogorodova, L.P., and Kupriyanova, I.I. (1984) Mineral equilibira in the system [BeO-Al_2O_3-SiO_2-H_2O]. International Geological Congress, 27th, 76.

Klementyeva, L.V. (1969) A find of bromellite in the U.S.S.R. Akademiya Nauk SSSR Doklady, 188, 152–154.

Komarova, G.N. (1974) Typomorphic minerals of aposkarn grei-

sens. In N.V. Pavlov, Ed., Problemy Endogennogo Rudoobrazovaniya, 222–234. Nauka, Moscow.

Kosals, Ya.A., Dmitriyeva, A.N., Arkipchuk, R.Z., and Gal'chenko, V.I. (1973) Temperature conditions and formation sequence in deposition of fluorite-phenakite-bertrandite ores. International Geology Review, 16, 1027–1936.

Kostryukov, V.N., Kosmilev, F.A., Samoryukov, O.P., Samoryukova, N.Ch., and Chesalina, L.A. (1977) The thermodynamic properties of beryllium hydroxide. Zhurnal Fizicheskoi Khimii, 51, 1015.

Kupriyanova, I.I. (1970) Paragenetic analysis of mineral associations in beryllium-bearing greisens. Zapiski Vsesoyunogo Mineralichekogo Obshchestva, 99, 277–285.

——— (1982) Dependence of parageneses of beryllium minerals on temperature and the activities of other components. Akademiya Nauk SSSR Doklady, 266, 714–718.

Kurepin, V.A. (1979) The thermodynamics of hydrous cordierite and cordierite-bearing mineral equilibria. Geokhimiya, 1979, 49–60.

Langer, K., and Schreyer, W. (1976) Apparent effects of water on the lattice geometry of cordierite: A discussion. American Mineralogist, 61, 1036–1040.

Levinson, A.A. (1962) Beryllium-fluorite mineralization at Aguacheile Mountain, Coahuila, Mexico. American Mineralogist, 47, 67–74.

Lindsey, D.A. (1979) Preliminary report on Tertiary volcanism and uranium mineralization in the Thomas Range and northern Drum Mountains, Juab County, Utah. U.S. Geological Survey Open-File Report 79–1076.

Martignole, J., and Sisi, J. (1981) Cordierite-garnet-H_2O equilibrium: A geologic thermometer, barometer, and water fugacity indicator. Contributions to Mineralogy and Petrology, 77, 38–46.

Martensson, C. (1960) Euklas und Bertrandit aus dem Feldspatpegmatit von Kolsva in Schweden. Neues Jahrbuch für Mineralogie Abhandlungen, 94, 1248–1252.

Meyer, C., and Hemley, J.J. (1967) Wall rock alteration. In H.L. Barnes, Ed. Geochemistry of hydrothermal ore deposits (1st edition), 166–235. Holt, Reinhart and Winston.

Miller, R.P., and Mercer, R.A. (1965) The high-temperature behavior of beryl melts and glasses. Mineralogical Magazine, 35, 250–276.

Mirwald, P.W., and Schreyer, W. (1977) Die stabile und metastabile Abbaureaktion von Mg-cordierit in Talk, Disthen und Quartz und ihre Abhangigkeit vom Gleichgewichtswassergehalt des Coridierits. Fortschritte der Mineralogie, 55, 95–97.

Mirwald, P.W., Maresch, W.V., and Schreyer, W. (1979) Der Wassergehalt von Mg-cordierit zwischen 500° und 800°C sowie 0.5 und 11 kbar. Fortschritte der Mineralogie, 57, 112–114.

Miyashiro, A. (1975) Metamorphism and metamorphic belts. John Wiley, New York.

Munson, R.A. (1967) High-temperature behavior of beryl and beryl melts at high pressure. American Ceramic Society Journal, 50, 669–670.

Nassau, K., and Wood, D.L. (1968) An examination of red beryl from Utah. American Mineralogist, 53, 801–807.

Newton, R.C. (1972) An experimental determination of the high-pressure stability limits of magnesian cordierite under wet and dry conditions. Journal of Geology, 80, 398–420.

Newton, R.C., and Wood, B.J. (1979) Thermodynamics of water in cordierite and some petrologic consequences of cordierite as a hydrous phase. Contributions to Mineralogy and Petrology, 68, 391–405.

Newton, R.C., Charlu, T.V., and Kleppa, O.J. (1974) A calorimetric investigation of the stability of anhydrous magnesium cordierite with application to granulite facies metamorphism. Contributions to Mineralogy and Petrology, 44, 295–311.

Okrusch, D.R. (1971) Zur Genese Von Chrysoberyl und Alexandit Lagerstatten. Eine Literaturubersicht. Zeitschrift Deutsche Gemmologischen Gesellschaft, 20, 114–124.

Olsen, D.R. (1971) Origin of topaz deposits near Ouro Preto, Minas Gerais, Brazil. Economic Geology, 66, 627–631.

Pavlova, I.G. (1965) Formation of phenakite from beryl in potassium metasomatism. Akademiya Nauk SSSR Doklady, 162, 147–150.

Perkins, D., III, Essene, E.J., Westrum, E.F., and Wall, V.J. (1979) New thermodynamic data for diaspore and their application to the system Al_2O_3-SiO_2-H_2O. American Mineralogist, 64, 1080–1090.

Reed, B.L., and Hemley, J.J. (1966) Occurrence of pyrophyllite in the Kekiktuk conglomerate, Brooks Range, northeastern Alaska. U.S. Geological Survey Professional Paper 550C, 162–166.

Rimstidt, J.D., and Barnes, H.L. (1980) The kinetics of silica-water reactions. Geochimica et Cosmochimica Acta, 44, 1683–1699.

Robie, R.A., Hemingway, B.S., and Fisher, J.R. (1978) Thermodynamic properties of minerals and related substances at 298.15 K and 1 bar (10^5 pascals) pressure and at higher temperatures. U.S. Geological Survey Bulletin 1452.

Robinson, G.R., Jr., Haas, J.L., Jr., Schafer, C.M., and Haselton, H.T. (1982) Thermodynamic and thermophysical properties of selected phases in the MgO-SiO_2-H_2O-CO_2, CaO-Al_2O_3-SiO_2-H_2O-CO_2, and Fe-FeO-Fe_2O_3-SiO_2 chemical systems, with special emphasis on the properties of basalts and their mineral components. U.S. Geological Survey Open-File Report 83-79.

Ross, M. (1964) Crystal chemistry of beryllium. U.S. Geological Survey Professional Paper 468.

Sainsbury, C.L. (1968) Geology and ore deposits of the central York Mountains, western Seward Peninsula, Alaska. U.S. Geological Survey Bulletin 1287.

Schlenker, J.L., Gibbs, G.V., Hill, E.G., Crews, S.S., and Myers, R.H. (1977) Thermal expansion coefficients for indialite, emerald, and beryl. Physics and Chemistry of Minerals, 1, 243–255.

Schreyer, W., and Yoder, H.S. (1964) The system Mg-cordierite–H_2O and related rocks. Neues Jahrbuch für Mineralogie Abhandlungen, 101, 271–342.

Schuiling, R.D., Verouwen, L., and van der Rijst, H. (1976) Gibbs energies of formation of zircon ($ZrSiO_4$), thorite ($ThSiO_4$), and phenacite (Be_2SiO_4). American Mineralogist, 61, 166–168.

Seck, H., and Okrusch, M. (1972) Phasenbeziehungen und Reaktionen im System BeO-Al_2O_3-SiO_2-H_2O. Fortschritte der Mineralogie, 50(1), 91–92.

Seitz, A., Rösler, U., and Schubert, K. (1950) The crystal structure of β-$Be(OH)_2$. Zeitschrift für Anorganische Chemie, 261, 94–105.

Skinner, B.J. (1966) Thermal expansion. In S.P. Clark, Jr., Ed. Handbook of physical constants (revised edition), 75–96. Geological Society of America Memoir 97.

Smirnov, V.I. (1977) Ore deposits of the U.S.S.R., Volume III. Pitman Publishing, San Francisco.

Stager, H.K. (1960) A new beryllium deposit at the Mount Wheeler mine, White Pine County, Nevada. U.S. Geological Survey Professional Paper 400-B, 70–71.

Stanek, J. (1978) Two types of beryllium pegmatites with gemstones in Northern Moravia, Czechoslovakia. XI. General International Mineralogical Association Meeting Novosibirsk Abstracts, II, 109.

Strand, T. (1953) Euclase from Iveland, occurring as an alteration product of beryl. Norsk Geologische Tidsskrift, 31, 1–5.

Strickland, J.D.H., and Parsons, T.R. (1972) A practical handbook of seawater analysis (2nd edition). Fisheries Research Board of Canada, Ottawa.

Stull, D.R., and Prophet, H. (1974) JANAF thermochemical tables (2nd edition). National Standards Reference Data Series, National Bureau of Standards (U.S.), 37.

Syromatnikov, F.V., Makarova, A.P., and Kupriyanova, I.I. (1971) Experimental study of the stability of beryl and phen-

akite under hydrothermal conditions. Zapiski Vsesoyungo Mineralogichekogo Obshchestva, 100, 222–225.

Van Valkenberg, A., and Weir, C.E. (1957) Beryl studies $3BeO \cdot Al_2O_3 \cdot 6SiO_2$. Geological Society of America Bulletin, 68, 1808–1809.

Vlasov, K.A., Ed. (1967) Geochemistry and mineralogy of rare elements and genetic types of their deposits. Volume II. Mineralogy of the rare elements. Volume III. Genetic types of rare element deposits. Nauka, Moscow (Israel Program for Scientific Translations, Jerusalem).

Walther, J.V., and Helgeson, H.C. (1977) Calculation of the thermodynamic properties of aqueous silica and the solubility of quartz and its polymorphs at high pressures and temperatures. American Journal of Science, 277, 1315–1351.

Woolfrey, J.L. (1973) Thermal expansion of $BeO \cdot Al_2O_3$, $BeO \cdot 3Al_2O_3$ and $3BeO \cdot 8Al_2O_3 \cdot 5MgO$. Australian Ceramic Society Journal, 9, 33.

Wood, B.J., and Walther, J.V. (1983) Rates of hydrothermal reactions. Science, 222, 413–415.

Wood, D.L., and Nassau, K. (1968) The characterization of beryl and emerald by infrared absorption spectroscopy. American Mineralogist, 53, 777–800.

Manuscript received April 8, 1985
Manuscript accepted October 10, 1985